

THE IMPACT OF HLA-DM ON PEPTIDE BINDING TO MHC CLASS II

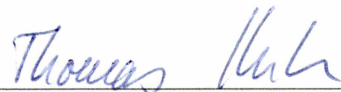
By

Megan Templeton

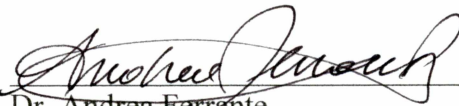
RECOMMENDED:



Dr. Karsten Hueffer
Advisory Committee Member



Dr. Thomas Kuhn
Advisory Committee Co-chair

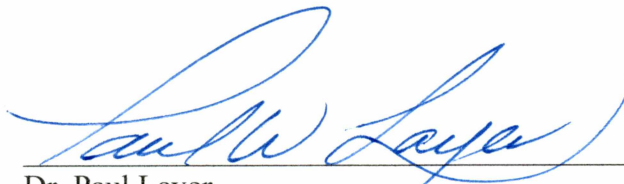


Dr. Andrea Ferrante
Advisory Committee Co-chair

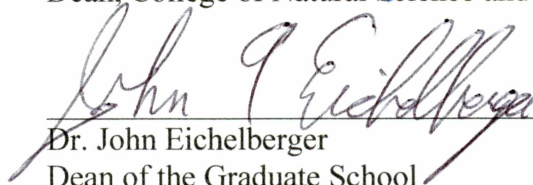


Dr. Thomas Green
Chair, Department of Chemistry and Biochemistry

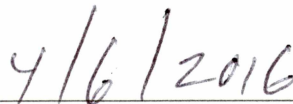
APPROVED:



Dr. Paul Layer
Dean, College of Natural Science and Mathematics



Dr. John Eichelberger
Dean of the Graduate School



Date

THE IMPACT OF HLA-DM ON PEPTIDE BINDING TO MHC CLASS II

A

THESIS

Presented to the Faculty
of the University of Alaska Fairbanks

in Partial Fulfillment of the Requirements
for the Degree of

MASTER OF SCIENCE

By

Megan Templeton, B.S.

Fairbanks, AK

May 2016

Abstract

Recognition of peptides bound to class II major histocompatibility complex (MHCII) molecules by T cell receptors of CD4⁺ T cells initiates an adaptive immune response. Analysis of the antigen presentation pathway indicates that elements of the epitope selection process are critical to generation of the peptide repertoire presented to T cells. Antigen presentation by dedicated cells (APCs) involves the intracellular fragmentation of protein antigens by cathepsins, binding of the derived peptide epitopes to MHCII with the participation of the peptide-editing molecule HLA-DM (DM), and subsequent transport to the surface for recognition. This thesis focuses on the energetics and structural flexibility of the peptide-MHCII complex, and their correlation with DM-susceptibility, to identify the criteria associated with the selection of peptides by APCs for subsequent presentation to T cells.

Using the human MHCII HLA-DR (DR), and peptides derived from influenza H3 HA₃₀₅₋₃₁₈ as test system, it was observed that, in the absence of DM, stable peptide binding is not reached through independent contributions of single-point interactions, but is a distributive process that involves the peptide-DR groove dyad in its entirety highlighting the inherent flexibility of the binding process. Here, DM mechanism is investigated in its ability to impact structural flexibility of the complex. Analysis of release from and binding to DR of a gamut of HA-derived peptides at two different levels of pH reveals that structural stability is reduced as a consequence of DM function. The results indicate that the outcome of DM activity is favoring the endurance of complexes with limited structural flexibility.

This page intentionally left blank

Table of Contents

	Page
Signature Page	i
Title Page	iii
Abstract	v
Table of Contents	vii
List of Figures	ix
List of Tables	ix
List of Appendices	ix
Chapter 1 An Introduction to Antigen Binding to MHC Molecules	1
1.1 Introduction to Major Histocompatibility Complex (MHC)	1
1.2 MHC Genetics	2
1.3 Antigen Presentation Pathways	2
1.4 Structure of MHC	3
1.5 Peptide Binding to MHC	4
1.6 Role of Non-classical MHCII Molecules	5
1.7 The Importance of Peptide Binding	6
1.8 Hypothesis	7
1.9 Figures	8
1.10 References	10
Chapter 2 HLA-DM Influences Epitope Selection by Favoring the Survival of Structurally Restrained Peptide-MHC Class II Complexes	13
2.1 Abstract	13
2.2 Introduction	14
2.3 Methods and Materials	15
2.4 Results	18
2.5 Discussion	20
2.6 Figures	23
2.7 Tables	29

2.8 Acknowledgements	30
2.9 References	31
Chapter 3 Conclusion.....	33
3.1 The Impact of DM on the Outcome of Epitope Selection.....	33
3.2 Future Directions.....	34
3.3 References	36

List of Figures

	Page
Figure 1.1 Exogenous Pathway of Antigen Presentation.....	8
Figure 1.2 Crystal Structure of DM and DR (PDB:4GBX).....	9
Figure 2.1 Fluorescence Polarization Dissociation at pH 6.4.....	23
Figure 2.2 Fluorescence Polarization Dissociation at pH 5.4.....	24
Figure 2.3 Cooperativity of Peptide Dissociation.....	25
Figure 2.4 Competitive Binding Assay at pH 6.4.....	26
Figure 2.5 Competitive Binding Assay at pH 5.4.....	27
Figure 2.6 Cooperativity of Peptide Binding.....	28
Figure A.1 Representative Raw ITC Data Titrating HA-derived Peptides into HLA-DR1 and β 81mut and the Fitted Binding Curves.....	59
Figure A.2 Far-UV CD and Thermal Stability Analysis of Empty MHCII Molecules and Different pMHCII Complexes.....	60
Figure A.3 MD Simulation of Empty MHCII and MHCII Bound to Different Peptides.....	61
Figure A.4 Structural Model of Peptide-dependent pMHCII Complex Modifications.....	62
Figure A.5 SPR Assay of DM Interaction with pMHCII Complexes.....	63
Figure A.6 FP-based Analysis of DM-susceptibility.....	64
Supplementary Figure A.1 SPR Assay of DM Interaction with pMHCII Complexes at pH 7.....	65

List of Tables

Table 2.1 List of Amino Acid Substitutions Applied to HA ₃₀₅₋₃₁₈	29
Table 2.2 Binding Affinity and Half-life Values.....	29
Table 2.3 Comparison to the Data in the Absence of DM.....	30
Table A.1 Binding Affinity and Thermodynamic Parameters.....	66
Table A.2 Midpoint Temperature, Enthalpy and Heat Capacity.....	66

List of Appendices

Appendix A The Thermodynamic Mechanism of Peptide-MHCII Complex Formation is a Determinant of Susceptibility to HLA-DM.....	37
Appendix B Permission from Lab Collaborators.....	73

This page intentionally left blank

Chapter 1 An Introduction to Antigen Binding to MHC Molecules

1.1 Introduction to Major Histocompatibility Complex (MHC)

An essential part of the immune system is to differentiate between self and non-self, a task that relies on the activity of white blood cells known as lymphocytes. The adaptive immune system, in particular, has evolved the capacity to recognize and respond to each pathogen in a specific fashion; such capacity differentiates the adaptive from the innate immune system, which features a quicker but more generic response. One subset of lymphocytes, B cells, is responsible for the generation of antibodies, which form the humoral branch of the adaptive response. A second subset of lymphocytes known as T cells constitutes the pillar of the cell-mediated immune response. These cells are characterized by their membrane receptor, known as T cell receptor (TCR). TCRs cannot directly bind pathogens; instead they can only interact with pathogen-derived peptides (antigens) when presented with molecules of the major histocompatibility complex (MHC) on other cells' membrane.

MHC binds peptides, the origin of which can be extremely variable, from self-proteins to viral components. MHC molecules are divided in three classes, with class I and II molecules being responsible for peptide presentation to T cells (1). T helper cells, or CD4⁺ T cells, recognize MHC class II molecules (MHCII) that are found on the surface of professional antigen presenting cells (APC). Variations of APC include: B cells, dendritic cells, macrophages, and epithelial cells of the thymus. Once CD4⁺ T cells are activated by APC, they proliferate, differentiate and they secrete small signaling proteins called cytokines that aid other immune cells. The cytotoxic T cells, or CD8⁺ T cells, recognize MHC class I molecules (MHCI), expressed on the surface of all nucleated cells. Once activated, CD8⁺ T cells will release granules containing perforin and granzymes that can destroy the targeted cell. MHCI bind and present peptides derived from intracellular proteins, while MHCII present peptides derived from extracellular proteins (2). The process of antigen presentation is an essential aspect to the generation of a specific T cell response, which is required to recognize and respond to infected or abnormal cells.

1.2 MHC Genetics

The importance of the MHC system became apparent in the context of organ transplantation, as it was clear that the basis of acceptance or rejection of a tissue is constituted by the matching between donor and recipient MHC alleles. Population analysis of MHC alleles has indicated that they are the most polymorphic proteins encoded by the human genome (3). The human MHC is named human leukocyte antigen (HLA), is encoded on chromosome 6 and the MHC locus contains 3.6 megabase pairs. The HLA system encompasses closely linked genes, which are inherited and is often associated with autoimmune diseases, like rheumatoid arthritis and diabetes (4). For each one of the two main HLA classes, three functional loci have been identified: the HLA class I includes, HLA-A, HLA-B and HLA-C loci, whereas the HLA class II includes, HLA-DR, HLA-DQ and HLA-DP. The allele we utilize in our experiments is HLA-DR1 (DR1). Although the evolution of the MHC system and its large polymorphism have led to an increased protection from infectious diseases, it is also likely that they are associated with an increased prevalence in autoimmune diseases (5).

1.3 Antigen Presentation Pathways

Antigen processing and presentation are the sequence of events that lead to the generation of peptides/MHC complexes for recognition by T cells. The antigenic peptides can derive from tumoral proteins, protein of intracellular pathogens or simply self-proteins targeted for removal. These peptides are usually presented by MHCI as a result of the endogenous pathway. If the peptides are generated from engulfed antigens, they are presented by MHCII at the end of the exogenous pathway.

In the endogenous pathway, the peptides originate from degraded or misfolded proteins from within the cell, which are ubiquitinated, marking them for proteasome degradation. The proteasome is a large, barrel-like protein complex with proteolytic activity, and peptidases (6). Polypeptides generated by the proteasome in the cytosol are transported into the endoplasmic reticulum (ER) through an ATP-dependent mechanism involving the transporter associated with antigen processing (TAP). MHCI molecules are synthesized within the ER and resident chaperones facilitate its appropriate folding. The MHC class I (heavy chain and β_2 -microglobulin) binds to the intraluminal face of TAP in a complex with the chaperones calreticulum and ERp57. Critical to this interaction is tapasin, which acts as a bridging molecule between the MHCI bound to the chaperone complex and TAP. Tapasin does not simply link

nascent MHCI molecules to TAP, but it is also required to facilitate binding of high affinity peptides to the MHCI. After peptide loading, MHCI dissociates from TAP and cluster at export sites on the ER membrane where they are selectively recruited into cargo vesicles for transport to the Golgi apparatus (7). MHCI then traffics through the Golgi apparatus to the plasma membrane.

The exogenous antigen processing begins within the ER of APCs, where the MHCII is synthesized as a heterodimer composed of $\alpha\beta$ subunits, which are then complexed with a trimer formed by three copies of the protein invariant chain (Ii). Binding to Ii prevents inappropriate endogenous peptides from infiltrating the binding groove, and provides the $\alpha\beta$ heterodimers with Ii sorting motifs for correct trafficking to the antigen processing compartments (8). The MHCII bound to Ii is transported directly or through an intermediate stop at the plasma membrane, to a specialized vesicle that is termed MHC class II compartment (MIIC) (9). When the Ii-MHCII complex reaches the acidic MIIC, the Ii is cleaved in a stepwise fashion by the proteolytic action of cathepsins (in particular cathepsin S and L), leaving a smaller peptide fragment named class II-associated invariant chain-derived peptide (CLIP) in the binding groove. A “non-classical” class II molecule, HLA-DM (DM) acts as an enzyme, promoting CLIP removal from the binding groove and antigenic peptide binding to MHCII. The entire process is shown in Figure 1.1, and represents the molecular machinery that entails the uptake of the pathogen by the APC, transportation within early and late endosomes through the cytoplasm, fusion within lysosomal vesicles and degradation via proteases. As classical and non-classical MHCII molecules populate these compartments, the MIIC is formed. Although MHCII loading can occur at any of these stages, the MIIC, with its acidic pH (~5.0 – 5.5), DM, and proteases, constitutes the ideal environment for peptide binding and DM activity. As kinetically and energetically stable peptide/MHCII complexes are formed, then they are transferred to the plasma membrane for subsequent recognition by CD4+ T cells.

1.4 Structure of MHC

MHCI molecules are composed of a single α chain, in which 3 domains can be identified ($\alpha 1$, $\alpha 2$ and $\alpha 3$) covalently associated to the polypeptide β_2 -microglobulin. The $\alpha 1$ and $\alpha 2$ domains are membrane-distal and form the site where peptides bind, which is also called the peptide binding groove. The MHCI binding groove is closed off, thus only peptides of 8 to 9 amino acids in length can be accommodated without kinks or bulges.

MHCII molecules are heterodimer proteins composed of two chains, α and β , in which four domains $\alpha 1 \alpha 2 \beta 1 \beta 2$ can be identified. The $\alpha 1$ and $\beta 1$ domains are membrane-distal regions forming the peptide binding site, whereas the membrane-proximal $\alpha 2$ and $\beta 2$ feature the typical Ig-like fold and are responsible for the anchoring to the membrane (APC cell surface or intracellular vesicle). The HLA class II peptide binding groove features a floor of eight strands of β sheet surrounded by two α -helices (10). Differently from MHCI, the MHCII has an open binding groove that can bind 12 to 17 amino acid residues. As peptides interact with the MHCII, they take a polyproline type II-like helix conformation, with side chains that interact with the binding groove of DR1 and 13 or more hydrogen bonds (H-bonds) established between the peptide backbone and the surrounding α -helices (11). Lining the floor of the binding groove is a group of pockets, referred to as P1, P4, P6 (sometimes P7) and P9, which are able to encapsulate peptide side chains. Various models have been put forth that account for the impact of the different pockets and H-bonds on peptide binding in the attempt to predict which sequences will be more likely to create an immune response.

1.5 Peptide Binding to MHC

Initial models describing peptide binding to MHC adopted the lock and key view, which has been historically used to describe ligand-receptor and enzyme-substrate interactions. More recently, the peptide binding process has been considered as a flexible event, during which the peptide folds itself and the binding groove to a low energy conformation. There are two approaches to model how peptide binds MHCII. The first model focuses on the role of the P1 anchor-pocket interaction in generating a stable complex. The P1 pocket is the largest and most hydrophobic pocket of the binding groove (in many, but not all alleles). This model originated from SDS gel studies where peptides able to fill the P1 pocket would preserve the MHCII dimeric conformation, whereas unbound or low affinity peptides would favor MHCII dissociation in two chains (12). These observations led to the idea that peptides with a lower affinity for MHCII are responsible for generating an empty or flexible P1 pocket that are more susceptible to DM action (13).

This model is opposed by a second model that indicates the overall dynamics of the peptide binding to MHCII as the primary target of DM recognition. Indeed, the second model postulates that DM susceptibility is based on the interactions and conformational changes that occur throughout the whole binding site as consequence peptide binding. A previous study showed that

multiple peptide substitutions at positions that do not interact with MHCII pockets affected binding affinity more than a single substitution at the P1 pocket; thus, when analyzing peptide binding, it is important to take into account the entire peptide (14). Subsequent studies found a way to measure the conformational flexibility of the MHCII binding peptide through cooperativity (15). The mechanism of peptide binding to MHCII and the role of DM in the selection of epitopes are yet to be determined.

1.6 Role of Non-classical MHCII Molecules

The polymorphism of DM was identified in cells with a defect in the process of peptide binding to MHCII (16). Subsequent analysis led to the realization that DM increased peptide dissociation from MHCII as well as increasing the peptide association with MHCII (17). However it became rapidly evident that DM does not act like a typical catalyst, in that it is unable to bind peptide, despite the MHCII-like structure. Instead, DM only interacts with MHCII.

In order to generate a T cell response, a peptide complexed to MHCII must be kinetically stable. DM enhances the binding of peptides that bind stably to MHCII, and it decreases the binding of unstable peptides (18). The measurement to determine DM susceptibility has frequently been that of peptide dissociation from MHCII in the presence of DM. Previous experiments have shown that peptides that quickly dissociate from MHCII were susceptible to DM, whereas the more stable peptide were less susceptible to DM (17). Recently it has been discovered that peptides that stay bound to MHCII for more than 75 hours will generate a specific T cell response, those that stay bound less than 10 hours will be unable to create a comparable response (19). Clearly, DM plays a large role in the endosomal selection of peptide/MHCII complexes destined to T cell recognition; DM with MHCII interaction can be better understood through the structural interpretation.

Initial studies indicated that DM is able to mediate CLIP removal from MHCII. Later work showed that DM activity is not limited to CLIP, in that it is able to catalyze exchange of antigenic peptides to select for a repertoire of kinetically and energetically stable peptide/MHCII complexes (20). The mechanism by which DM interacts with MHCII and alters peptide binding and release has not been fully elucidated yet. For many years it was impossible to determine a crystal structure of MHCII interacting with DM; in the last four years studies have overcome the previous quandary through various methods. Pos and colleagues (21) were able to capture the

structure of DM interacting with DR1 bound to a partial HA peptide missing the P-1, P1, and P2 positions (leaving the P1 pocket empty) and linked by a disulfide bond at the P6 pocket. Visualizing the structure was accomplished by linking DR1 with DM by their β subunits with sortase A (21). The resolved crystal structure is shown in Figure 1.2. This structure provided confirmation to prior studies adopting indirect approaches, which suggested that DM interacts with DR1 at the N-terminal by targeting the α -helix.

Another non-classical MHC molecule that is involved in the exogenous pathway of antigen presentation is HLA-DO (DO). Although still debated, it appears that the role of DO would be that of inhibiting DM, by competing with MHCII for binding to the same location on DM (22). Structurally, DO is similar to MHCII, and it would interact with DM via the same molecular region involved in the binding of MHCII to DM. The amount of DO is regulated by transcription, and it appears that there is a higher concentration of DM within the MIIC, therefore DM would be partially involved in DM-DO complexes and the remaining DM would be amenable to interact with classical MHCII (23).

1.7 The Importance of Peptide Binding

Explaining peptide binding to MHC and the subsequent presentation to T cells has a wide variety of implications, from understanding the immune response to a typical pathogen infection to being able to determine better options for peptide-based vaccinations. The clinical importance of antigen presentation can be seen when self peptides bind MHCII, potentially leading to autoimmune disorders in the context of reduced tolerance: for instance certain defects in HLA-DQ alleles can lead to celiac disease and type 1 diabetes (24). During cancer, tumoral cells have been shown to hijack antigen presentation to avoid detection from T cells, and some malignant tumors down regulate MHC expression with the same purpose (25).

Considering the breadth of the potential antigenic repertoire, and the polymorphism of HLA molecules, being able to predict if certain peptides will bind specific alleles would allow development of peptide-based vaccines, identification of self-epitopes correlated with autoimmunity, and could be adopted for epidemiological purposes. It would be nearly impossible, costly and time-consuming, to experimentally measure binding of all possible amino acid combinations for all known alleles. To overcome the limitations of *in vitro* measurement, *in silico* peptide binding prediction algorithms have been engineered. There are two approaches to predict peptides, a direct method, which predicts epitopes based on what the T cell receptor will

recognize (these have been less successful), or an indirect method, based on which epitope will bind the MHC (26). Reliable peptide binding prediction algorithms would greatly benefit vaccine development, from the seasonal influenza to the Ebola virus (27, 28). However, the precision of the current prediction models is questionable, in particular for MHCII binding: one study showed that T cell response to predicted *Pseudomonas* exotoxin five epitopes were correctly predicted, however another four were missed entirely (29). An explanation for some of the missing epitopes might be that algorithms do not take into account DM action in the process of prediction or the role of MHCII structural flexibility during peptide binding. A better understanding of DM activity during antigen presentation, and its inclusion in prediction algorithms would dramatically increase our ability to engineer reliable T cell epitopes mapping models.

1.8 Hypothesis

The purpose of our experiments is to investigate DM function and the impact it has on the structural flexibility of the peptide/MHCII complex. Previous studies have shown that measuring cooperativity of interactions within the binding groove is a suitable approach to better probe the peptide binding process (30). On the basis of our prior analysis of cooperativity in peptide binding to and release from MHCII in the absence of DM, and the structural and kinetic studies of DM activity reported above, we predict that DM will favor the survival of peptide/MHCII complexes in which structural flexibility is limited. We will test our hypothesis by quantitating cooperative effects on binding to and release from the human MHCII HLA-DR1 as determined with cycle-mutated peptides derived from the sequence of the influenza peptide HA₃₀₅₋₃₁₈ (31, 32).

1.9 Figures

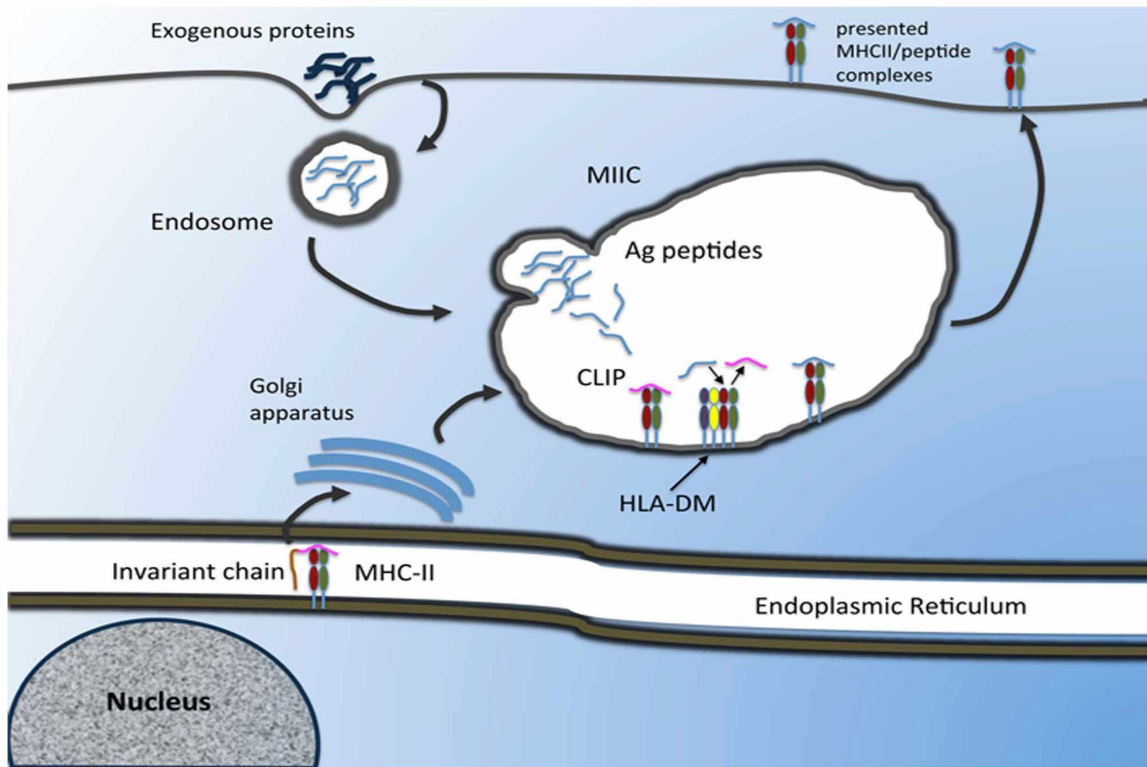


Figure 1.1 Exogenous Pathway of Antigen Presentation

Within antigen presenting cells, exogenous proteins are cleaved and the resulting peptides are loaded onto the MHCII, transported to the surface of the cell, and presented to CD4+ T cells.

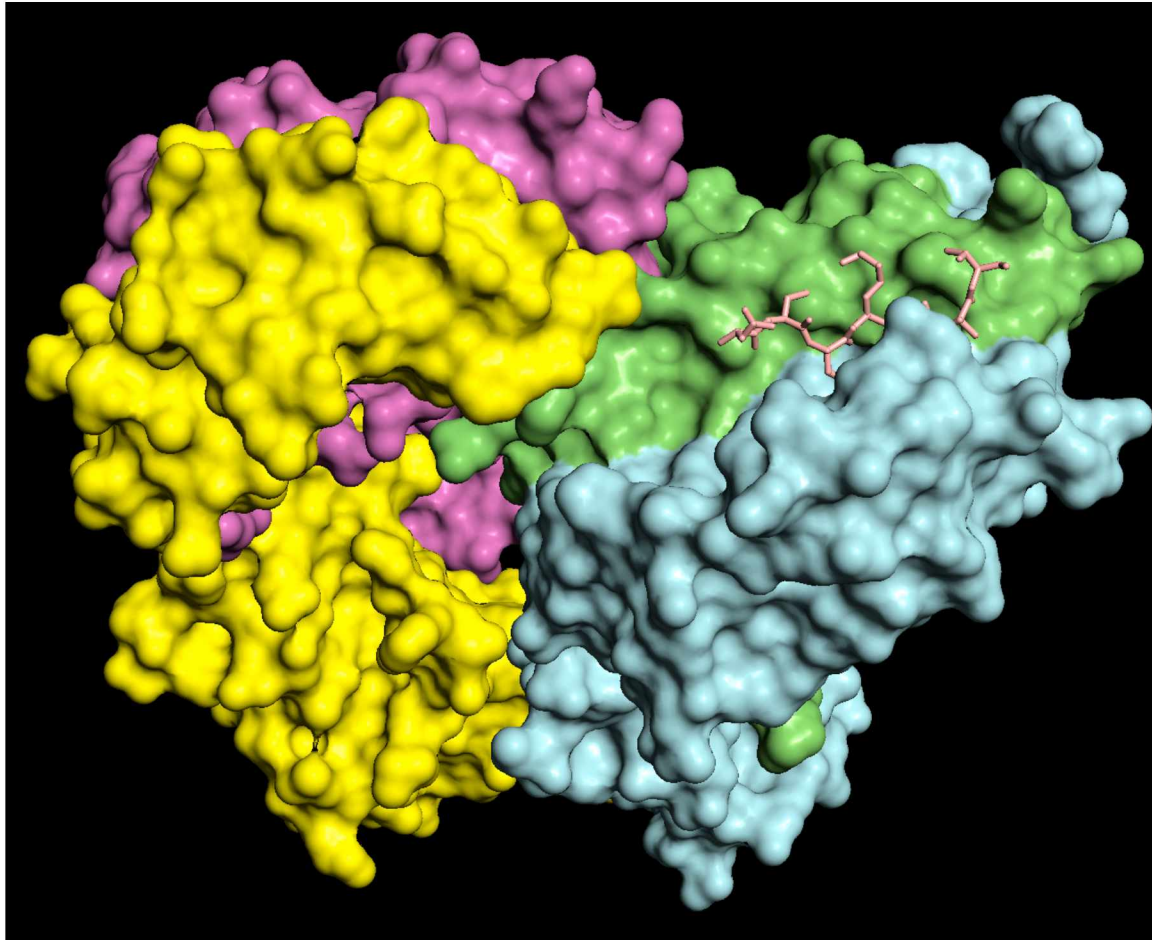


Figure 1.2 Crystal Structure of DM and DR (PDB: 4GBX)

DM α chain is shown in magenta, the DM β chain in yellow, the DR α chain in green, and DR β subunit in blue. An HA peptide lacking three N-terminal residues is shown in pink. The structure of PDB: 4GBX was modeled in PyMol, coordinates are taken from Pos, et al (21).

1.10 References

1. Paul WE. *Fundamental Immunology*: Wolters Kluwer Health; 2012.
2. Blum JS, Wearsch PA, Cresswell P. Pathways of antigen processing. *Annu Rev Immunol*. 2013 Jan; 31(1): 443-73.
3. Beck S, Trowsdale J. The human major histocompatibility complex: lessons from the DNA sequence. *Annu Rev Genomics Hum Genet*. 2000; 1(1): 117-37.
4. Consortium. Complete sequence and gene map of a human major histocompatibility complex. *Nature*. 1999 Oct; 401(6756): 921-3.
5. Gruen JR, Weissman SM. Evolving views of the major histocompatibility complex. *Blood*. 1997 Dec; 90(11): 4252-65.
6. Lázaro S, Gamarra D, Del Val M. Proteolytic enzymes involved in MHC class I antigen processing: a guerrilla army that partners with the proteasome. *Molecular Immunology*. 2015 May; 68: 72-76.
7. Raghavan M, Cid ND, Rizvi SM, Peters LR. MHC class I assembly: out and about. *Trends Immunol*. 2008 Sep; 29(9): 436-43.
8. Pieters J. MHC class II restricted antigen presentation. *Curr Opin Immunol*. 1997 Feb; 9(1): 89-96.
9. Katz JF, Stebbins C, Ettore A, Sant AJ. Invariant chain and DM edit self-peptide presentation by major histocompatibility complex (MHC) class II molecules. *The Journal of Experimental Medicine*. 1996 Nov; 184(5): 1747-53.
10. Brown JH, Jardetzky TS, Gorga JC, Stern LJ, Urban RG, Strominger JL, et al. Three-dimensional structure of the human class II histocompatibility antigen HLA-DR1. *Nature*. 1993 Jul; 364(6432): 33-9.
11. Stern LJ, Brown JH, Jardetzky TS, Gorga JC, Urban RG, Strominger JL, et al. Crystal structure of the human class II MHC protein HLA-DR1 complexed with an influenza virus peptide. *Nature*. 1994 Mar; 368(6468): 215-21.
12. McFarland BJ, Beeson C. Binding interactions between peptides and proteins of the class II major histocompatibility complex. *Med Res Rev*. 2002 Mar; 22(2): 168-203.
13. Chou CL, Sadegh-Nasser S. HLA-DM Recognizes the flexible conformation of major histocompatibility complex class II. *The Journal of Experimental Medicine*. 2000 Dec; 192(12): 1697-706.

14. Anderson MW, Gorski J. Cutting edge: TCR contacts as anchors: effects on affinity and HLA-DM stability. *J Immunol*. 2003 Dec; 171(11): 5683-7.
15. Anderson MW, Gorski J. Cooperativity during the formation of peptide/MHC class II complexes. *Biochemistry*. 2005 Apr; 44(15): 5617-24.
16. Mellins E, Smith L, Arp B, Cotner T, Celis E, Pious D. Defective processing and presentation of exogenous antigens in mutants with normal HLA class II genes. *Nature*. 1990 Jan; 343(6253): 71-4.
17. Sloan VS, Cameron P, Porter G, Gammon M, Amaya M, Mellins E, et al. Mediation by HLA-DM of dissociation of peptides from HLA-DR. *Nature*. 1995 Jun; 375(6534):802-6.
18. Sant AJ, Chaves FA, Jenks SA, Richards KA, Menges P, Weaver JM, et al. The relationship between immunodominance, DM editing, and the kinetic stability of MHC class II: peptide complexes. *Immunol Rev*. 2005 Oct; 207(1): 261-78.
19. Sant AJ, Chaves FA, Leddon SA, Tung J. The control of the specificity of CD4 T cell responses: thresholds, breakpoints, and ceilings. *Front Immunology*. 2013 Oct; 4: 340.
20. Kropshofer H, Arndt SO, Moldenhauer G, Hämmerling GJ, Vogt AB. HLA-DM acts as a molecular chaperone and rescues empty HLA-DR molecules at lysosomal pH. *Immunity*. 1997 Mar; 6(3): 293-302.
21. Pos W, Sethi DK, Wucherpfennig KW. Mechanisms of peptide repertoire selection by HLA-DM. *Trends in Immunology*. 2013 Oct; 34(10): 495-501.
22. Guce AI, Mortimer SE, Yoon T, Painter CA, Jiang W, Mellins ED, et al. HLA-DO acts as a substrate mimic to inhibit HLA-DM by a competitive mechanism. *Nat Struct Mol Biol*. 2013 Dec; 20(1): 90-8.
23. Denzin LK, Cresswell P. Sibling rivalry: competition between MHC class II family members inhibits immunity. *Nat Struct Mol Biol*. 2013 Jan; 20(1): 7-10.
24. Busch R, De Riva A, Hadjinicolaou AV, Jiang W, Hou T, Mellins ED. On the perils of poor editing: regulation of peptide loading by HLA-DQ and H2-A molecules associated with celiac disease and type 1 diabetes. *Expert Rev Mol Med*. 2012 Jul.
25. Seliger B, Maeurer MJ, Ferrone S. Antigen-processing machinery breakdown and tumor growth. *Immunol Today*. 2000 Sep; 21(9): 455-64.

26. Goodswen SJ, Kennedy PJ, Ellis JT. Enhancing *in silico* protein-based vaccine discovery for eukaryotic pathogens using predicted peptide-MHC binding and peptide conservation scores. *PloS One*. 2014 Dec; 9(12): 1-20.
27. Khan MA, Hossain MU, Rakib-Uz-Zaman SM, Morshed MN. Epitope-based peptide vaccine design and target site depiction against Ebola viruses: an immunoinformatics study. *Scand J Immunol*. 2015 Jul; 82(1): 25-34.
28. Shamsavandi S, Ebrahimi M, Sadeghi K, Mahravani H. Design of a heterosubtypic epitope-based peptide vaccine fused with hemokinin-1 against influenza viruses. *Virology*. 2015 Jun; 53(3): 200-7.
29. Mazor R, Tai CH, Lee B, Pastan I. Poor correlation between T-cell activation assays and HLA-DR binding prediction algorithms in an immunogenic fragment of *Pseudomonas* exotoxin A. *J Immunol Methods*. 2015 Oct; 533: 10-20.
30. Ferrante A, Gorski J. Cooperativity of hydrophobic anchor interactions: evidence for epitope selection by MHC class II as a folding process. *J Immunol*. 2007 Jul; 178: 7181-89.
31. Horovitz A, Fersht AR. Strategy for analysing the co-operativity of intramolecular interactions in peptides and proteins. *J Mol Biol*. 1990 Aug; 214(3): 613-7.
32. Horovitz A, Fersht AR. Co-operative interactions during protein folding. *J Mol Biol*. 1992 Apr; 224(3): 733-40.

Chapter 2 HLA-DM Influences Epitope Selection by Favoring the Survival of Structurally Restrained Peptide-MHC Class II Complexes¹

2.1 Abstract

HLA-DM (DM) plays a critical role in generating the peptide-MHC class II (MHCII) repertoire expressed on the surface of antigen presenting cells and recognized by CD4+ T cells. The action of DM requires acidic conditions, and its catalytic effect increases as pH lowers. We have previously shown that at pH 7.4 in the absence of DM, peptide binding to and release from MHCII is a flexible process as evidenced by cooperativity. Cooperativity indicates that peptide binding does not rely on independent contributions of single-point interactions, instead multiple interactions along the peptide binding groove determine binding in a non-additive fashion. However, it is still unclear whether the system of flexibility represented by cooperativity of binding is a function of DM activity. To address this issue, we have measured the cooperative effects involved in the interaction between a panel of cycle-mutated peptides derived from the sequence of the influenza peptide HA₃₀₅₋₃₁₈ and the human MHCII allele HLA-DR1 (DR1) in the presence of DM. Peptide release studies and competitive binding assays performed at pH 5.4 and pH 6.4 show that cooperativity in peptide binding is reduced and this effect is magnified at low pH, suggesting that this is a DM-dependent phenomenon. Taken together, our results indicate the outcome of DM activity is favoring the survival of complexes with limited structural flexibility.

¹ Templeton, M.L., and A. Ferrante. 2015. HLA-DM impacts epitope selection by favoring the survival of structurally restrained peptide-MHC class II complexes. Prepared for Cellular & Molecular Immunology.

² Ferrante A., Templeton, M., Hoffman, M., and Castellini, M. The Thermodynamic Mechanism

2.2 Introduction

During an immunization or infection, exogenous antigens are engulfed and processed by antigen presenting cells (APC) within endosomal compartments. Peptides generated via proteolytic cleavage by cathepsins are then selected for binding to MHC class II (MHCII) molecules, and the resulting complexes are relocated to the cell membrane and presented to CD4⁺ T cells (1). The process of which peptide is selected for binding to MHCII is key to consequential recognition by the T cell receptor to initiate a CD4⁺ T cell response. The MHCII is an $\alpha\beta$ heterodimer synthesized bound to the protein invariant chain (Ii), which prevents binding of protein prematurely; the Ii MHCII complex is then transported to a specialized vesicle known as MHC class II compartment (MIIC) (2). Once inside the low pH of MIIC, Ii is cleaved by proteasomes into a smaller peptide termed class II-associated invariant chain peptide (CLIP) that remains within the binding groove of MHCII. For many MHCII alleles HLA-DM (DM), a non-classical MHCII molecule, facilitates the removal of CLIP, enabling peptides generated from exogenous proteins to compete for binding. It is known that DM promotes the decision by the endosomal machinery as to which peptides will be selected and presented by the MHCII. The peptide bound to MHCII (pMHCII) repertoire, in the presence of DM, is skewed in favor of energetically stable complexes (3). The molecular mechanism behind this process, however, is poorly understood.

The interaction between the peptides and MHCII has been extensively studied. The specific MHCII allele HLA-DR1 (DR1) is the focus of this study; the binding groove is composed of a β sheet, surrounded by two α -helices (4). As with many MHCII proteins, DR1 binds with what are referred to as anchor interactions at the P1, P4, P6, and P9 positions within the binding groove, where the pockets are deep and hydrophobic (5). In addition to these largely solvent inaccessible interactions, positions with smaller pockets or shelves in the binding site accommodating the P2, P3, P7, and P10 residues are recognized as minor or auxiliary anchors. Finally, there is a conserved array of hydrogen bonds (H-bonds) from side chains in the MHCII to the main chain atoms of the peptide.

The crystal structure of DR1 in complex with DM, as well as mutagenesis studies, have shown that DM interacts at the N-terminal of the binding groove in the region adjacent to the P1 and P2 pocket, possibly a displaced form of the α -helix of DR1 which moves away from the binding groove (6). This observation implies that the peptide residue that is occupying the P1

pocket will have a lasting effect on peptide stability in the presence of DM. The peptide that is binding to the MHCII needs to have a high affinity and long half-life in order to stay bound long enough on the surface of the APC to be recognized by the CD4+ T cell. There has been an indication that DM consistently seems to favor these high affinity (K_D) and longer half-life ($t_{1/2}$) peptides to bind the DR1, rather than their unstable peptide counterparts (7). These experiments aim to determine the function of DM by means of dissociation and binding kinetics.

Our past analysis performed at physiological pH and in the absence of DM has evidenced that pMHCII complex affinity and kinetic stability do not rely on independent contributions from single-point interactions (8). Rather, during peptide binding, all sources of binding energy are coupled, in that the inability of binding at one position reduces the likelihood of binding at any other positions. Therefore the impact of destabilizing one interaction on the overall binding process is not constant, but is a function of the total binding energy available to the complex, this is termed cooperativity. Subsequently, we analyzed the thermodynamics of the peptide binding reaction this can be seen in the paper attached in the appendix (9). The collected observations suggest a thermodynamic-structural model where peptides binding DR1 optimize the available interactions through search of conformational space, and as they bind, system flexibility is restrained.

Here we analyze DM function under the hypothesis that its interaction with the pMHCII complex impacts the structural stability of the same complex. We measure cooperative effects involved in the interaction between a panel of cycle-mutated peptides derived from the influenza peptide HA₃₀₅₋₃₁₈ and DR1 in the presence of DM at different conditions of pH (10, 11). Taken together, our results indicate that DM activity is favoring the survival of complexes with limited structural flexibility.

2.3 Methods and Materials

Peptide Synthesis

Peptides derived from the sequence GPKYVKQNTLKLAT, representing residues 305-318 of the hemagglutinin (HA) protein from influenza A virus (H3 subtype), are listed in Table 2.1 (4). The N-terminal Gly facilitated labeling. Side chains in the HA peptide are numbered relative to the P1Y residue. N-terminal labeling with FAM or LC-LC Biotin was performed on the resin before deprotection, and then peptides were cleaved and purified by HPLC and

confirmed by MALDITOF mass spectrometry. Peptides were provided by AnaSpec Inc. Fremont, CA.

Expression and purification of recombinant soluble DR1 protein

Recombinant soluble empty (peptide free) DR1 was produced and purified by ioGenetics (Madison, WI) from a stably transfected *CHO* mammalian cell line with a proprietary retroviral vector transduction system essentially as described for antibodies. The genes code for proteins of 192 (α) and 198 (β) residues, which terminate just before the beginning of the predicted transmembrane spans (residues 193-197 and 199-203 respectively). The vector was designed to generate a poly-His tag at the C-terminus of the expressed protein. DR-expressing clones were selected and expanded. His-tagged DR1 proteins were purified with a His-trap HP column coupled to an ÄKTAFPLC chromatography system, and buffer exchanged into PBS (7 mM Na^+/K^+ phosphate, 135 mM NaCl, pH 7.4) using centrifugal ultra-filtration (Amicon). Soluble FLAG-tagged DM was isolated from a stably transfected *Drosophila S2* cell line as described by Arvis Proteins Inc. To avoid contamination with FLAG peptide, DM elution from the resin was performed with 0.1 M glycine HCl, pH 3.5. Both DR1 and DM proteins were purified and buffer exchanged into K/Na-phosphate buffer (1.47 mM KH_2PO_4 , 8.1 mM Na_2HPO_4 , 135 mM NaCl, 2.7 mM KCl, pH 7.4) using centrifugal ultra-filtration (Amicon). Purity (>95%) was confirmed by SDS-PAGE stained with GelCode Blue Stain Reagent (Pierce).

Fluorescence polarization (FP) dissociation measurements

DR/peptide complexes were formed by incubating 1 μM DR1 with a 10-fold excess of FAM-labeled peptide in PBS @ 37°C over night, and purified from unbound peptide by buffer exchange into PBS (pH 7.4) @ 4°C with a Centricon YM-30 spin filter (Amicon) previously treated with MES. 100 nM of purified DR1/peptide complexes were incubated with 100-fold excess of unlabeled HA 305-318 peptide to prevent rebinding of freshly dissociated peptide in the presence of 3-fold excess DM. Reactions were performed @ 37°C in 50 mM sodium citrate/sodium phosphate buffer at pH 5.4 or MES buffer at pH 6.4 and were covered with mineral oil to prevent evaporation. Fluorescence polarization was monitored for 580 and 800 minutes after addition of the peptide and DM until equilibrium was reached. To avoid non-specific adherence of the protein, black polystyrene 96-well plates were used (Corning). Measurements were performed using a Wallac VICTOR counter (PerkinElmer Wallac) with the

excitation wavelength=485 nm and emission wavelength=535 nm. Specific control groups included (a) protein only, (b) peptide only, and (c) buffer only, and were used for background correction. FP and anisotropy are mathematically related ways of expressing parallel:perpendicular emission ratios and are easily interconverted. Although FP is approximately linear with respect to the ratio of free:bound peptide, FP was converted to anisotropy (which is exactly linear) by the following equation $A = 2 * FP / (3 - FP)$ where A is anisotropy and FP indicates fluorescence polarization in mP units. Anisotropy values were fitted either according to a single- or a bi- exponential decay model to find the $t_{1/2}$ where 50% of the complex was remaining. Each experiment was performed in triplicate, and the reported dissociation rate reflects the mean \pm SD of three independent experiments.

Equilibrium-based competition binding assay

Relative binding affinities were determined by a competitive binding assay essentially as described previously (12, 13). DR1 (40 or 80 nm) was incubated with equimolar amount of biotinylated HA peptide and three-fold DM in binding buffers (0.1% BSA, 0.01% Tween 20, 0.1 mg/ml 4-(2-aminoethyl)-benzene sulfonyl fluoride, 0.1 mM iodoacetamide, 5 mM EDTA, 0.02% NaN₃) at pH 5.4 (with sodium citrate) or pH 6.4 (2-(N-morpholino)ethanesulfonic acid, MES) in the presence of varying amounts of inhibitor peptides for 3 days at 37°C. The incubation time ensures the majority (>65%) of DR1 protein participates in the peptide binding reaction to reach equilibrium. Bound biotinylated peptide was detected using a solid-phase immunoassay and Eu²⁺-labeled streptavidin. Plates were read using a Wallac VICTOR counter (PerkinElmer Wallac). Data were fit to a logistic equation $y = a / [1 + (x/x_0)^b]$. IC50 values were obtained from the curve fit of the binding data and converted to K_D values by using the equation $K_D = (IC50) / (1 + [b_{HA}] / K_{D,bHA})$ in which $K_{D,bHA}$ was set equal to 57.8 nM at pH 5.4 and 77.6 nM at pH 6.4 on the basis of the results of the direct binding of bio-HA peptide to DR1. Each point represents the mean and SD of three independent experiments performed in triplicate. Because pMHCII binding represents a multistep reaction, the IC50 for a competitive binding assay may not be directly proportional to the K_D (14). Although this can be offset by long incubations relative to half-life, we study low affinity peptides where half-lives are impossible to determine. Therefore, the values of affinity reported herein should be considered as apparent K_D values.

Calculation of cooperative effects

We view cooperativity in pMHCII folding as the enhancement in binding or dissociation that arises in a second (or subsequent) interaction as a result of the primary interaction (8). This definition has been used by others in the context of protein folding or ligand binding (10, 15). We used a multiple substitution strategy previously used to identify interacting partners during protein folding (3, 9). To normalize the $t_{1/2}$ and K_D values of a given pMHCII complex, we define the effect of each substitution as the ratio of the substituted measurement over that of the DR1/wild-type (wt)HA value ($\Delta t_{1/2}$ for stability or ΔK_D for affinity). Normalization of the measurements to that of the DR1/wt HA complex also allows for comparison of cooperativity measures in stability, which is measured directly, and affinity, which is measured indirectly.

For calculating cooperativity, the effect of multiple substitutions is measured directly (observed value). The expected value for a combination of substitutions is calculated as the product of the individual substitutions [e.g., $\Delta t_{1/2, x,y} = (\Delta t_{1/2,x}) \times (\Delta t_{1/2,y})$]. For peptides with three substitutions, the expected value would be the product of all the different substitutions [e.g., $\Delta t_{1/2, x,y,z} = (\Delta t_{1/2,x}) \times (\Delta t_{1/2,y}) \times (\Delta t_{1/2,z})$]. The cooperativity is the ratio of the expected to observed ($C = \text{exp/obs}$) values for either $\Delta t_{1/2}$ or ΔK_D . A value of 1 for the ratio of expected/observed indicates no cooperativity, for it would suggest independent energetic contribution in binding and/or release from each substitution. Cooperativity is evidenced when the ratio of expected/observed is not equal to 1.

2.4 Results

To test the effect of DM on cooperativity of the pMHCII interaction, thus structural flexibility, mutations were made at P1, P2, P4, and P7 position. The peptide generated via cycle mutation applied to the sequence of the HA₃₀₅₋₃₁₈ peptide are reported in Table 2.1. For the P1 position, it has been previously shown that changing P1 to Val decreases the stability of the DR1/HA complex in the presence of SDS (16). Glu at P4 instead of Gln is expected to destabilize the formation of an H-bond with DR1 Gln9, whereas Arg introduces a basic residue at a position that prefers acidic side chains. Structural modeling revealed that two of these substitutions could potentially interfere with formation of H-bonds normally observed in the HA/DR1 structure. Indeed, the P2 and P7 Asp substitutions are located at positions in the peptide/DR1 interface in which rotation of the side chain around the α -carbon can directly destabilize H-bonds to the peptide backbone. Alternatively, these substitutions may indirectly

lead to destabilization by facilitating solvent entry into the binding groove. Each substitution would provide an interaction sufficient for the formation of the complex, but when combined with substitutions at the other positions could reveal a measureable cooperativity during the interaction.

Cooperativity is a measurement of the flexibility when peptide binds to MHCII. During previous experiments in the absence of DM at pH 7.4, cooperativity was shown to contribute to complex stability (8). To determine the effect of DM on the energetics of the complex, we examined complex stability by determining the dissociation rate at both pH 6.4, Figure 2.1, and at pH 5.4, Figure 2.2. The individual data points of Figure 2.1 and 2.2 represent the mean $t_{1/2}$ of three independent experiments, the individual peptide $t_{1/2}$ values can be seen in Table 2.2. Each individual substitution resulted in small effects on the dissociation rate, except the PIV substitution, and the multiple substitutions had variable effects. These results are different than what is observed in the absence of DM as can be seen in Table 2.3, where the general trend is that DM shortens the $t_{1/2}$ and this is more noticeable at the lower pH where DM is more active (17). To test the relative effect of peptide release, each singly substituted complex was calculated with respect to the stability of the unsubstituted DR1/HA complex. If the contribution of each substitution to complex stability were independent, then the effect of multiple substitutions would equal the product of their individual effects on stability. The ratio of observed to expected stability gives the cooperativity. In Figure 2.3 we show that cooperative effects are larger at pH 5.4 than at pH 6.4, although the R^2 values show that the curve fitting is not the best representative for the cooperativity data, yielding an $R^2 = 0.471$ at pH 5.4 and $R^2 = 0.251$ at pH 6.4. This trend is unexpected, since we would have predicted a different trend in the cooperativity compared to $t_{1/2}$ plot. Several explanations for this deviation might be that, the short $t_{1/2}$ for PIV could disrupt some of the multiple V substitutions of cooperativity; another could suggest that there are more structural conformations occurring during dissociation than what we were expecting. So we decided to calculate cooperativity on peptide binding, which are derived at equilibrium.

To assess the effect of DM on peptide binding, equilibrium-based competitive binding assays were completed at pH 6.4, as seen in Figure 2.4, and pH 5.4 reported in Figure 2.5. From the curve fits it is possible to determine the IC50 of each substituted peptide, which can be converted into a relative binding affinity (K_D) by using the Cheng-Prusoff equation as described in the

methods. There were two peptides P1,2,4 VDR and P1,2,4,7 VDEG that lost binding capabilities at pH 5.4. The relative K_D values that were calculated from these figures are reported in Table 2.2. From these values cooperative effects on peptide binding for multiple substituted peptides can be determined as the ratio between the observed K_D (normalized over K_D of wt HA peptide) and the expected normalized K_D , which is calculated by multiplying the normalized K_D from individual substitutions. Each point on Figure 2.4 and 2.5 was the result of the mean of three independent experiments, and error bars were the standard deviation of these three experiments from the mean. Compared to the peptide affinities in the absence of DM shown in Table 2.3, DM decreases the value of K_D and this has implications for the stability of the complex (17).

The results of the cooperativity can be seen in Figure 2.6. The plot shows that as the pH decreases the slope of cooperativity is smaller. The fit of cooperativity compared to binding affinity at pH 5.4 has a slope of 0.772 with an R^2 of 0.927, while the fit for pH 6.4 has a slope of 0.898 with an $R^2=0.975$. These results indicate that cooperativity is reduced in the presence of DM, and that this effect increases as the pH lowers, indicating that this is a DM-dependent phenomenon.

2.5 Discussion

Despite its importance in epitope selection, the mechanism of DM-mediated peptide exchange remains unclear. In this work, we analyze DM activity under the hypothesis that its action affects the structural flexibility involved in the pMHCII interaction. To test this hypothesis we adopted a multiple substitution strategy, previously described for the study of cooperative interactions in protein folding (15). Through this approach, one can construct a series of higher order mutant cycles to analyze the impact of different peptide substitutions relative to the wt HA sequence on complex energetics. We have adopted such a method in the case of intrinsic peptide binding to and release from DR1 (8, 18) and we have used it with a limited subset of peptides in the presence of DM to explore the impact of a specific DR1 mutation on DM function (19). Here we extend such studies to a broader library of peptides carrying a different set of mutations and we perform release and binding assays at two pH conditions to probe the impact of DM on cooperative effects, and thus system flexibility. We found that DM activity decreases cooperative effects in peptide binding, and such an effect is magnified at more acidic conditions, in keeping with the known pH-dependence of DM function.

The crystallographic studies of pMHCII complexes have been important to infer general structural principles of peptide binding (6). However they indicate a stereotypic structure for these proteins, whereas biochemical data suggest the existence of alternate conformers as a function of pH and presence of peptide. Investigations aimed at better understanding which regions of the MHCII are involved in changes upon binding indicate that the α -subunit 3_{10} helical region and the adjacent extended strand, the $\beta 2$ Ig-like domain, and the pronounced kink in the β -subunit helical region $\beta 62-71$ are the most subject to conformational heterogeneity, also for the bound state (20). Evidently, MHCII proteins have a degree of structural flexibility that can affect the interaction with the peptide and possibly decide the structure of the resulting complex, a feature not readily evident in the crystal structures. Such flexibility is evidenced by thermodynamic properties, such as cooperativity and entropy-enthalpy compensation, and we have shown that DM interacts with complexes where the formation is associated with smaller entropic penalty and greater conformational lability, as described in our paper attached in the appendix (9). The current data provide an important insight into the mechanism of DM function, indicating that the outcome of the DM/pMHCII interaction is to favor the formation of complexes with limited structural flexibility (reduced cooperativity); moreover there is no preferential position along the peptide binding groove determining the magnitude of DM effect.

Whereas the interpretation of the binding assays appears straightforward, DM-mediated dissociation experiments show cooperativity trends that would not be easily derived by inference from the intrinsic dissociation studies. Indeed, off-rates of the multiple substituted peptides were slower than expected at pH 6.4, but particularly at pH 5.4. This observation seems to conflict with the increasing cooperativity measured for multiple substituted peptides as a result of DM activity and decreasing pH. One explanation for this apparent paradox is that DM may affect peptide on-rate as well as peptide release, thus the overall cooperative effect observed at the equilibrium in our binding experiments reflects DM action on both directions of reaction. With this regard, a recent work has been published showing that the association of peptides with MHCII in the presence of DM have faster kinetics than the MHCII alone, and presented multiple possibilities for the on-rate as well as the off-rate (21).

A second explanation for the different cooperativity trends may relate to the various partial reactions occurring during the release assays monitored in real time, which are not evident in the binding assays measured at equilibrium, as they are a function of state. During DM-

mediated off-rates, it is possible that the addition of unlabeled competitor peptide in excess exerts an effect on complex kinetic stability in the presence of DM, and such effect is independent from the characteristics of the bound peptide. Moreover, as FAM-peptide is released from DR and substituted by unlabeled competitor, new complexes are formed, which might interact with DM; the activity of DM on unlabeled peptide/DR complexes, may cause the changes in DM/FAM-peptide/DR stoichiometry over time, affecting the contribution of DM to FAM-peptide release.

On the basis of the current results, and previously published observations, we propose a model of DM mechanism where DM interacts preferentially with complexes featuring a significant conformational lability, in particular in the aforementioned regions, reflecting the thermodynamic mechanism adopted by peptide and MHCII to form a complex. Upon interaction, DM would form an intermediate with MHCII that binds peptide with faster kinetics than MHCII in the absence of DM (21). Such an intermediate would facilitate peptide exchange, consequently accelerating the identification of those ligands, which can form a complex with limited structural flexibility. Once a complex with reduced conformational stability is formed it would dissociate from DM and relocate to the membrane for T cell recognition.

Although we think that the above model provides a solid explanation for the observations reported by our and other groups, other questions about DM mechanism are still open. For instance, it is not clear how a DM-pMHCII intermediate resolves to generate an exchanged pMHCII complex. We still do not know whether the exchanging peptide competes with the pre-bound mainly via P1 pocket, or through interactions throughout the entire peptide binding groove. Our distributed model of peptide binding would favor the latter, but it is possible that this is a peptide or allele phenomenon. Moreover, it would be important to understand how peptide sequence determines the ability to be exchanged onto MHCII during antigen presentation. We have proposed a model involving a tetramolecular DM-MHCII-two peptide intermediate based on kinetics and spin-label studies (22), however further analysis is required to fully describe this important step of the epitope selection process.

2.6 Figures

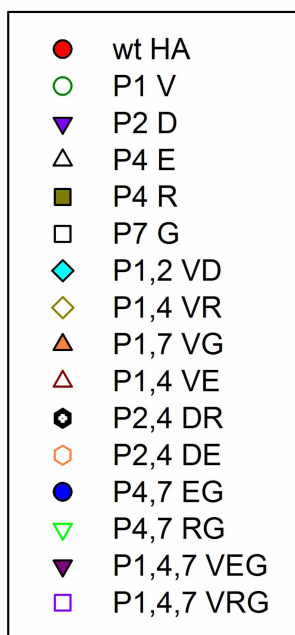
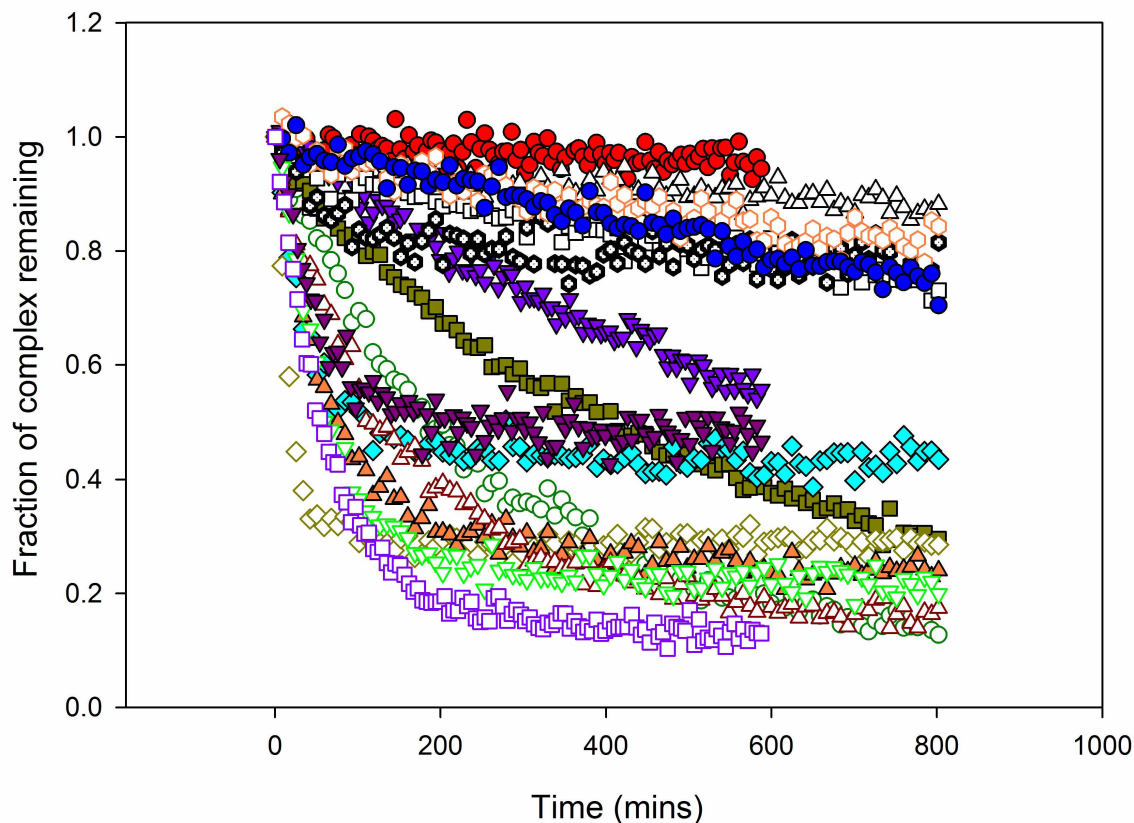
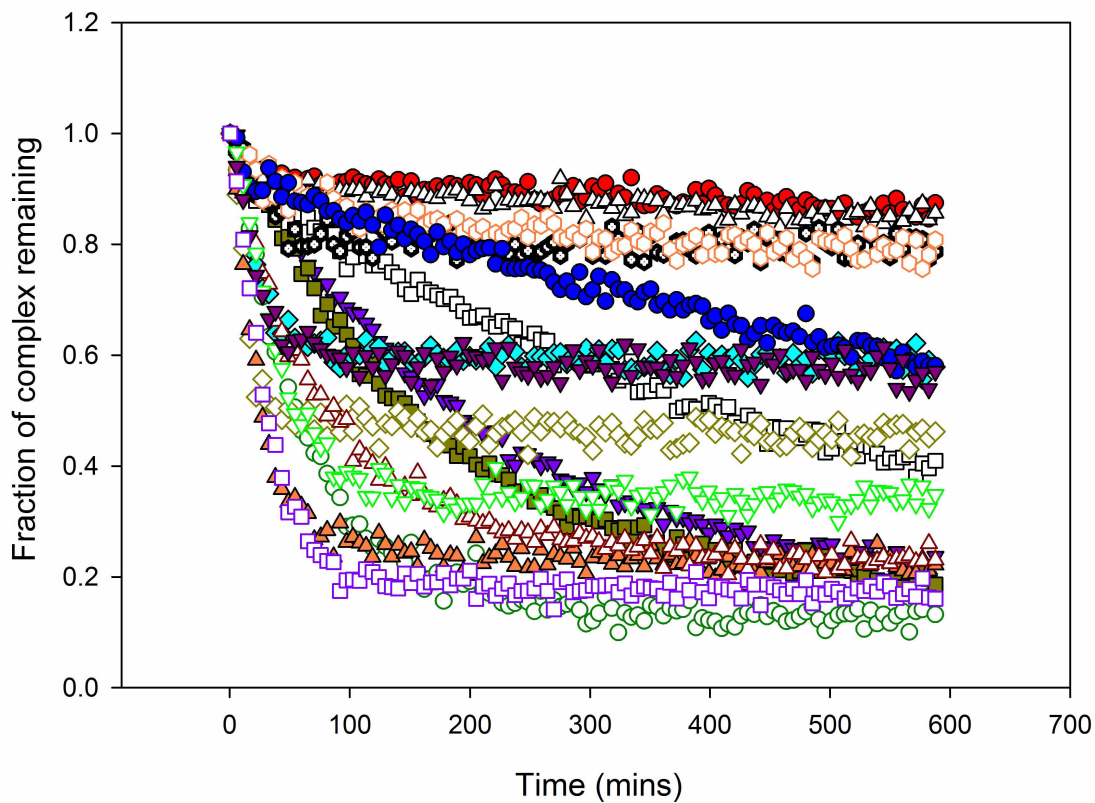


Figure 2.1 Fluorescence Polarization Dissociation at pH 6.4
 Dissociation rates of pMHCII complexes. Data are expressed as the fraction of complex remaining relative to $t = 0$. Reactions were performed in triplicate, and data series represent one of three independent experiments. The protocol was changed part way through the pH 6.4 experiments, which is why data for wt HA, D, VEG, VRG extend only to 580 minutes on this graph.



- wt HA
- P1 V
- ▼ P2 D
- △ P4 E
- P4 R
- P7 G
- ◆ P1,2 VD
- ◇ P1,4 VR
- ▲ P1,7 VG
- △ P1,4 VE
- ◊ P2,4 DR
- P2,4 DE
- P4,7 EG
- ▽ P4,7 RG
- ▼ P1,4,7 VEG
- P1,4,7 VRG

Figure 2.2 Fluorescence Polarization Dissociation at pH 5.4

DM-mediated dissociation rates of pMHCII complexes at pH 5.4. Data are expressed as the fraction of complex remaining relative to $t = 0$.

Reactions were performed in triplicate, and data series represent one of three independent experiments.

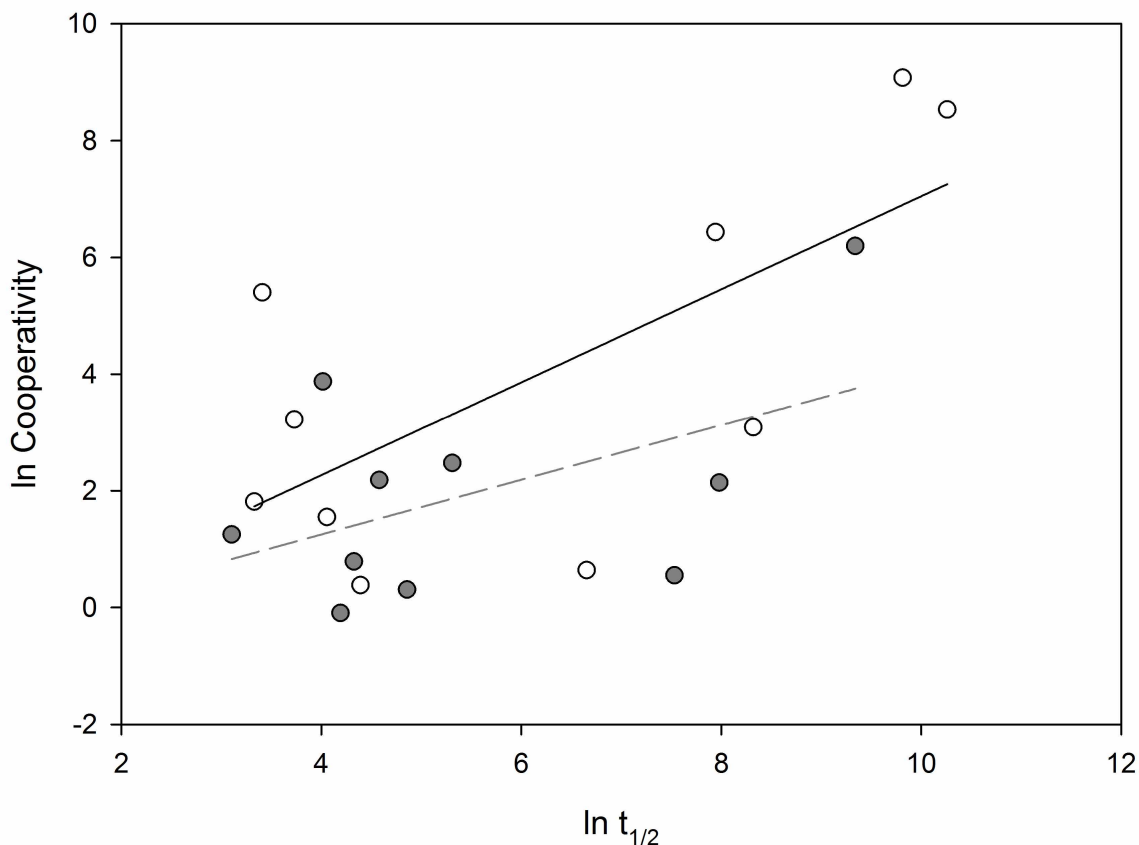
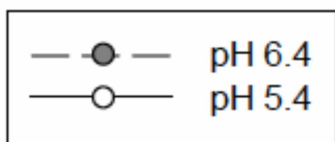


Figure 2.3 Cooperativity of Peptide Dissociation



Natural log (ln) plot of cooperativity (observed/expected $t_{1/2}$) vs.

DM-mediated dissociation rate for each DR1/peptide complex

tested at pH 6.4 (gray dot, dashed lines) and at pH 5.4 (white dots,

solid lines). Since we defined cooperativity C as the ratio of the observed to expected values for

$\Delta t_{1/2}$, and $t_{1/2}$ is directly proportional to stability, the cooperative effect is negative if $0 \leq C < 1$,

while if $C > 1$ the cooperative effect is positive. In the ln plot, positive cooperativity in stability is

indicated on the y-axis by values > 0 and negative cooperativity by values < 0 . Lines indicate the

fit of the data to a linear regression (pH 6.4: slope = 0.469, $R^2=0.251$; pH 5.4: slope 0.797, $R^2=0.471$).

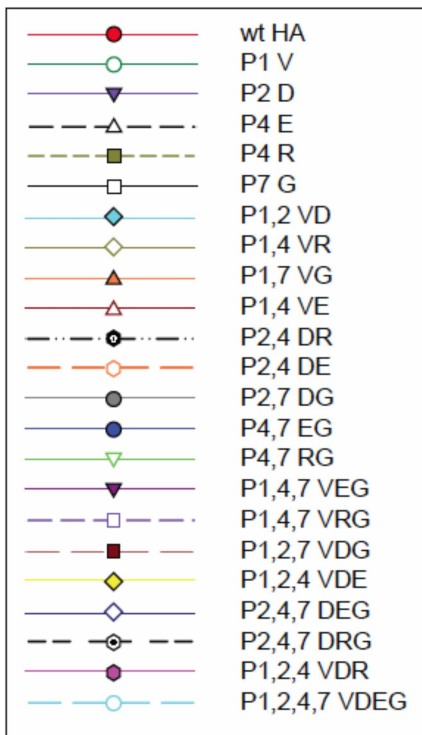
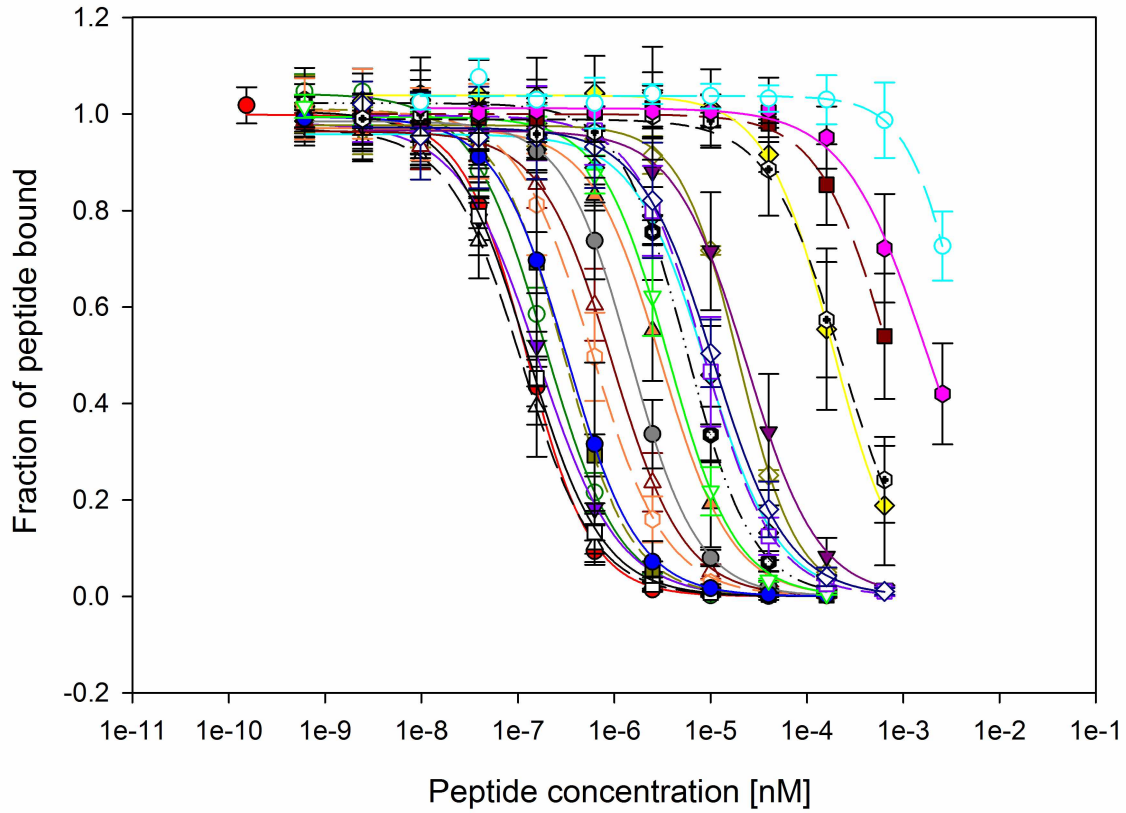


Figure 2.4 Competitive Binding Assay at pH 6.4

Competition binding analysis of P1, P2, P4 and P7

substituted HA peptide variants to DR1. Data represent the mean and SD of three independent experiments. Lines indicate the fit of the data to a logistic equation. The K_D values for each peptide are reported in Table 2.2.

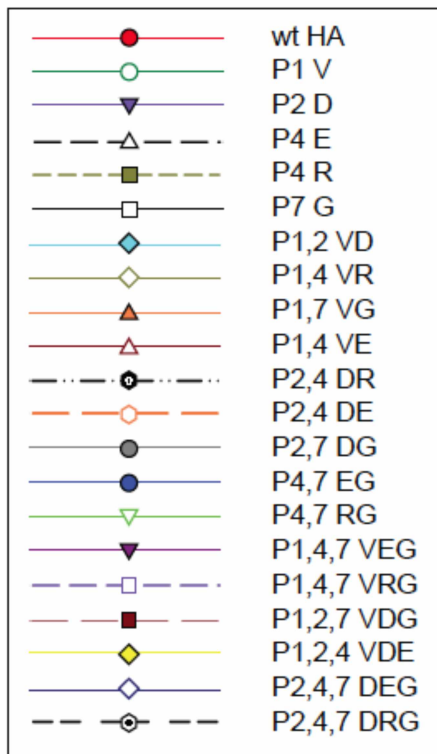
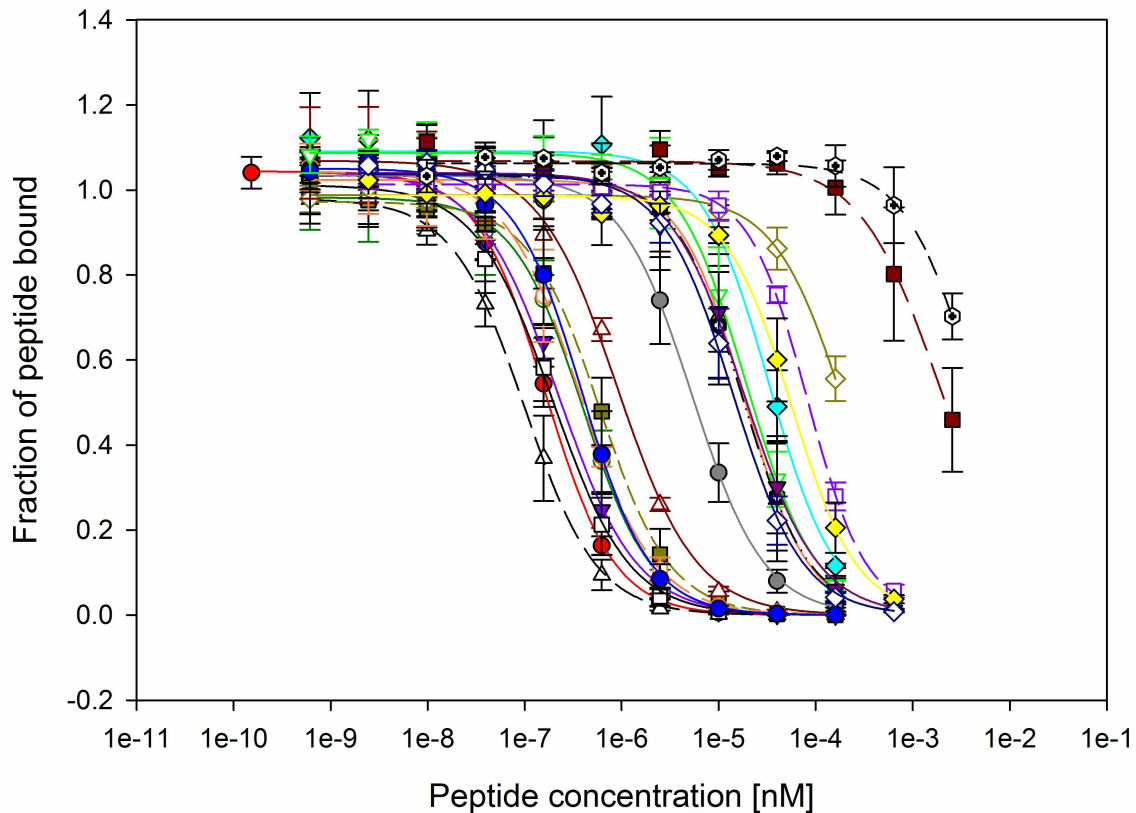


Figure 2.5 Competitive Binding Assay at pH 5.4

Competition binding analysis of P1, P2, P4 and P7

substituted HA peptide variants to DR1. Data represent the mean and SD of three independent experiments. Lines indicate the fit of the data to a logistic equation. The K_D values for each peptide are reported in Table 2.2.

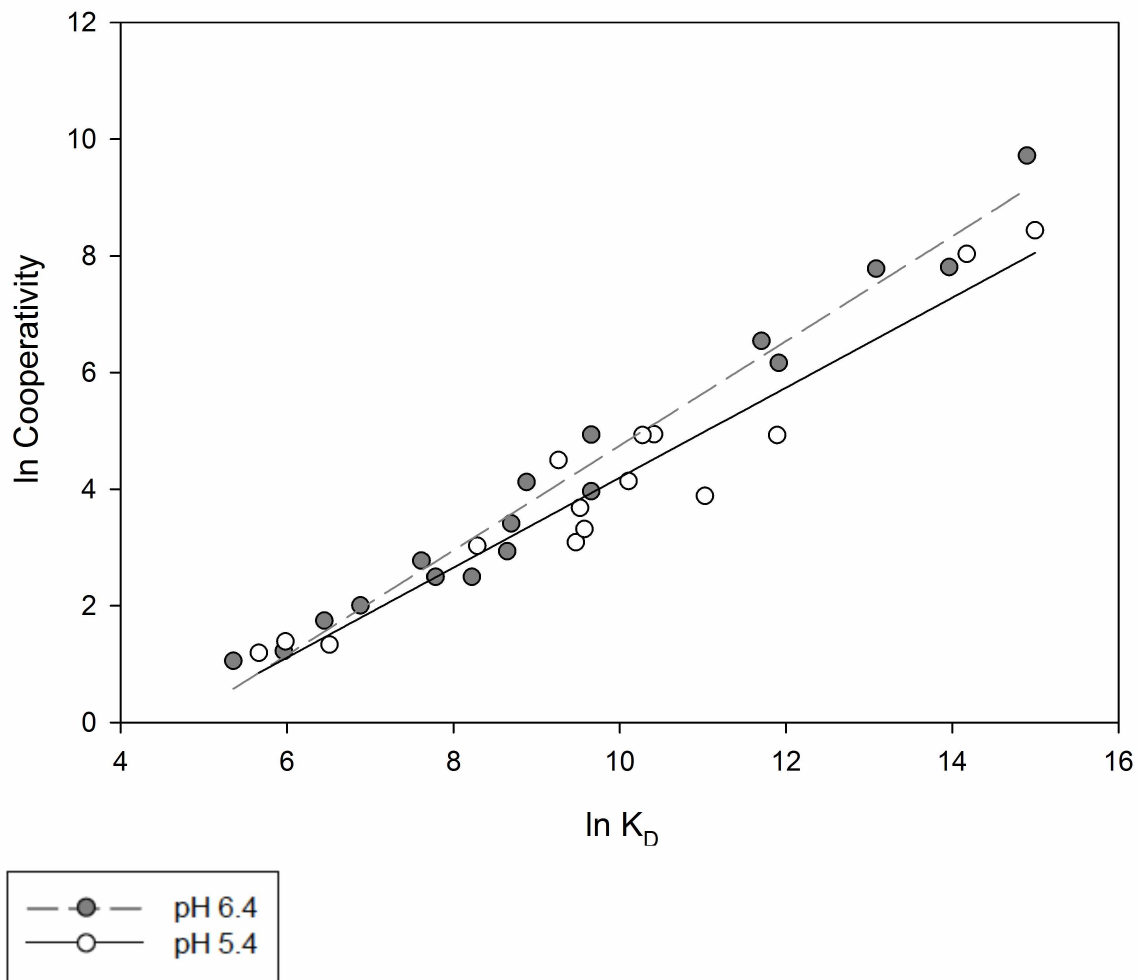


Figure 2.6 Cooperativity of Peptide Binding

Natural log (ln) plot of cooperativity (observed/expected K_D) vs. DM-mediated dissociation constant for each DR1/peptide complex tested at pH 6.4 (gray dot, dashed lines) and at pH 5.4 (white dots, solid lines). Since we defined cooperativity C as the ratio of the observed to expected values for ΔK_D , and K_D is inversely proportional to binding affinity, the cooperative effect is positive if $0 \leq C < 1$, while if $C > 1$ the cooperative effect is positive. In the ln plot, positive cooperativity in stability is indicated on the y-axis by values < 0 and negative cooperativity by values > 0 . Lines indicate the fit of the data to a linear regression (pH 6.4: slope = 0.898, $R^2=0.975$; pH 5.4: slope = 0.772; $R^2=0.927$).

2.7 Tables

Table 2.1 List of Amino Acid Substitutions Applied to HA₃₀₅₋₃₁₈

Shown here is the wt HA₃₀₅₋₃₁₉ sequence (PKYVKQNTLKLAT, with the G at the N-terminal added for labeling purposes). P1, P2, P4, P7 refer to the peptide positions interacting with the DR1 pockets lining the binding groove. Underneath the original sequence the amino acids adopted for the cycle mutation are indicated. These substitutions lead to 22 unique peptides.

			P1	P2				P4						P7	
G	P	K	Y	V	K	Q	N	T	L	K	L	A	T		
			V	D				E						G	
									R						

Table 2.2 Binding Affinity and Half-life Values

Affinity and dissociation rate of substituted peptide/HLA-DR1 complexes. N/A: not available.

Peptide	K_D at 6.4	K_D at 5.4	$t_{1/2}$ (mins) at 6.4	$t_{1/2}$ (mins) at 5.4
wt HA	82	121	12100	5000
P1 V	125	291	191	55
P2 D	129	162	696	189
P4 E	72	74	6000	4973
P4 R	194	441	404	150
P7 G	83	143	2174	411
P2,7 DG	975	3,969	N/A	N/A
P2,4 DE	388	396	2927	4111
P2,4 DR	3,718	12,970	11400	28600
P1,2 VR	15,620	146,500	22	42
P1,2 VD	5,968	24,500	97	18300
P1,4 VE	632	673	128	81
P4,7 EG	212	287	1870	775
P4,7 RG	2,399	14,400	666	58
P1,7 VG	2,032	13,650	76	28
P1,2,4 VDE	121,200	33,330	N/A	N/A
P1,4,7 VEG	15,590	29,020	202	2815
P2,4,7 DEG	7,173	10,520	N/A	N/A
P1,4,7 VRG	5,683	61,420	55	30
P2,4,7 DRG	149,200	3,258,000	N/A	N/A
P1,2,7 VDG	481,400	1,433,000	N/A	N/A
P1,2,4 VDR	1,159,000	No binding	N/A	N/A
P1,2,4,7 VDEG	2,954,000	No binding	N/A	N/A

Table 2.3 Comparison to Data in the Absence of DM

DM+/- DM- for both affinity and dissociation rate of substituted peptide/HLA-DR1 complexes

N/A: not available.

Peptide	K_D at 6.4	K_D at 5.4	$t_{1/2}$ (mins) at 6.4	$t_{1/2}$ (mins) at 5.4
wt HA	2.21	2.89	0.302	0.014
P1 V	0.91	2.16	0.130	0.035
P2 D	1.34	1.55	0.190	0.026
P4 E	1.01	1.57	0.001	0.029
P4 R	2.95	2.64	0.357	0.103
P7 G	1.11	1.03	0.237	0.032
P2,7 DG	3.57	12.28	N/A	N/A
P2,4 DE	2.16	1.51	0.722	0.201
P2,4 DR	5.17	5.45	0.829	3.57
P1,2 VR	2.90	16.40	0.655	1.02
P1,2 VD	1.40	3.80	0.487	20.15
P1,4 VE	2.12	2.00	0.138	0.035
P4,7 EG	2.43	1.95	0.265	0.044
P4,7 RG	5.30	7.05	0.396	0.316
P1,7 VG	3.69	9.86	0.419	0.176
P1,2,4 VDE	6.42	6.22	N/A	N/A
P1,4,7 VEG	2.23	4.05	0.466	1.14
P2,4,7 DEG	1.49	6.24	N/A	N/A
P1,4,7 VRG	3.79	8.80	0.362	0.258
P2,4,7 DRG	2.87	27.26	N/A	N/A
P1,2,7 VDG	2.97	9.69	N/A	N/A
P1,2,4 VDR	3.37	N/A	N/A	N/A
P1,2,4,7 VDEG	2.00	N/A	N/A	N/A

2.8 Acknowledgements

We would like to thank our lab collaborators Megan Hoffman and Maggie Castellini that provided the data of the DM negative research.

2.9 References

1. Watts C, Powis, S. Pathways of antigen processing and presentation. *Rev Immunogenet.* 1999 Jan; 1: 60 - 74.
2. Katz JF, Stebbins C, Ettore A, Sant AJ. Invariant chain and DM edit self-peptide presentation by major histocompatibility complex (MHC) class II molecules. *The Journal of Experimental Medicine.* 1996 Nov; 184(5): 1747-53.
3. Chou CL, Sadegh-Nasseri S. HLA-DM Recognizes the flexible conformation of major histocompatibility complex class II. *The Journal of Experimental Medicine.* 2000 Dec; 192(12): 1697-706.
4. Stern LJ, Brown JH, Jardetzky TS, Gorga JC, Urban RG, Strominger JL, et al. Crystal structure of the human class II MHC protein HLA-DR1 complexed with an influenza virus peptide. *Nature.* 1994 Mar; 368(6468): 215-21.
5. Nelson CA, Fremont DH. Structural principles of MHC class II antigen presentation. *Rev Immunogen.* 1999 Jan; 1(1): 47 - 59.
6. Pos W, Sethi DK, Wucherpfennig KW. Mechanisms of peptide repertoire selection by HLA-DM. *Trends in Immunology.* 2013 Oct; 34(10): 495-501.
7. Blum JS, Wearsch PA, Cresswell P. Pathways of antigen processing. *Annu Rev Immunol.* 2013 Jan; 31(1): 443-73.
8. Anderson MW, Gorski J. Cooperativity during the formation of peptide/MHC class II complexes. *Biochemistry.* 2005 Apr; 44(15): 5617-24.
9. Ferrante A, Templeton M, Hoffman M, Castellini MJ. The thermodynamic mechanism of peptide-MHC class II complex formation is a determinant of susceptibility to HLA-DM. *J Immunol.* 2015 Aug; 195(3): 1251-61.
10. Horovitz A, Fersht AR. Strategy for analysing the co-operativity of intramolecular interactions in peptides and proteins. *J Mol Biol.* 1990 Aug; 214(3): 613-7.
11. Horovitz A, Fersht AR. Co-operative interactions during protein folding. *J Mol Biol.* 1992 Apr; 224(3): 733-40.
12. Jensen PE, Moore JC, Lukacher AE. A europium fluoroimmunoassay for measuring peptide binding to MHC class I molecules. *Journal of Immunological Methods.* 1998 June; 215(1-2): 71-80.

13. Yin L, Stern LJ. A novel method to measure HLA-DM-susceptibility of peptides bound to MHC class II molecules based on peptide binding competition assay and differential IC(50) determination. *Journal of Immunological Methods*. 2014 Apr; 406: 21-33.
14. Beeson C, McConnell HM. Kinetic intermediates in the reactions between peptides and proteins of major histocompatibility complex class II. *PNAS*. 1994 Sep; 91(19): 8842-5.
15. Creighton TE. Protein folding: an unfolding story. *Current Biology*. 1995 Apr; 5(4): 353-6.
16. Ferrante A, Gorski J. Enthalpy–entropy compensation and cooperativity as thermodynamic epiphenomena of structural flexibility in ligand–receptor interactions. *Journal of Molecular Biology*. 2012 Apr; 417(5): 454-67.
17. Ferrante A, Hoffman, Megan, Castellini, Maggie. The effect of pH changes on HA peptide binding to MHC class II. *Nature Immunology*. Manuscript in preparation.
18. Ferrante A, Gorski J. Cooperativity of hydrophobic anchor interactions: evidence for epitope selection by MHC class II as a folding process. *J Immunol*. 2007 Jul; 178: 7181-89.
19. Ferrante A, Gorski J. Cutting edge: HLA-DM-mediated peptide exchange functions normally on MHC class II-peptide complexes that have been weakened by elimination of a conserved hydrogen bond. *J Immunol*. 2010 Jan; 184:1153-8.
20. Painter CA, Stern LJ. Conformational variation in structures of classical and nonclassical MHCII proteins and functional implications. *Immunological reviews*. 2012 Nov; 250(1): 144-57.
21. Yin L, Maben ZJ, Becerra A, Stern LJ. Evaluating the role of HLA-DM in MHC class II-peptide association reactions. *J Immunol*. 2015 Jul; 195(2): 706-16.
22. Ferrante A, Anderson MW, Klug CS, Gorski J. HLA-DM mediates epitope selection by a “compare-exchange” mechanism when a potential peptide pool is available. *PloS one*. 2008 Nov; 3(11): e3722.

Chapter 3 Conclusion

3.1 The Impact of DM on the Outcome of Epitope Selection

The response that develops from T cells recognizing epitopes bound to MHC is a significant part of the immune defense against pathogens. Exogenous antigen presentation within APC is a well-understood system, with the exception of the exact mechanism of how DM regulates the binding of peptides to MHCII. The aim of the research presented here was to determine the function of DM and its impact on the process of peptide binding to MHCII. Understanding the basic action of DM has the potential to aid in the prediction of the epitope selection process. During the course of these experiments, the hypothesis was tested that DM functions by favoring the survival of peptide/MHCII complexes in which structural flexibility is limited. To confirm this hypothesis, cycle-mutated HA_{305–318} peptides were examined using fluorescence polarization to test peptide dissociation and competitive binding assays to examine peptide binding. Cooperativity was calculated as a proxy for structural flexibility in the system in the attempt to develop insights into DM activity.

The results of peptide dissociation experiments in the presence of DM gave an unexpected measurement of cooperativity. Analysis of off-rate data for individual peptides however, revealed that DM decreased the $t_{1/2}$ as compared to experiments where DM was absent, also in the case of multiple-substituted peptides which appear to unfold more slowly than what expected on the basis of single substitutions. The measurements from peptide dissociation do not provide a clear insight into DM action; this result could be due to the likelihood that there are multiple states of binding of the peptide to MHC, with different susceptibility to DM (1). An additional reason for the unanticipated results of release experiments is the possible sequestration of DM by complexes formed by the unlabeled competitor peptide, once the latter displaces the originally bound fluorescently labeled peptide. Although the kinetics of this interaction is not monitored by the FP signal, it affects the kinetics of the fluo-peptide release from MHCII by altering the complex:DM ratio. With this regard, a recent work has been published showing that the association of peptides with MHCII in the presence of DM have faster kinetics than the MHCII alone, and presented multiple possibilities for the on-rate as well as the off-rate (2). On the other side, the competitive binding assays measured at the equilibrium indicated that cooperativity is reduced in the presence of DM. Since cooperativity is a measurement of flexibility, we interpret these observations as an indication that DM is more likely to act on

pMHCII complexes that have a larger conformational lability, resulting in the survival of less flexible complexes. However, further work is needed to determine a more exact model, which may reconcile the binding data with the release experiments.

These sets of experiments provided new information on the mechanism of DM action during the peptide binding process. A better model of peptide binding has implications on the general knowledge of the typical pathogen infection, and it would also provide improved options for peptide-based vaccinations. The *in silico* approach of creating peptide binding prediction algorithms is promising, but shows significant shortcomings in accuracy (3). A more detailed understanding of DM action would greatly help the process of predicting peptide binding to MHCII. We expect to gain decisive insights in DM activity by coupling isothermal titration calorimetry (ITC) analysis of the DM-MHCII-peptide interaction with structural analysis of complex flexibility with high-resolution spectroscopy (EPR or TR-FA).

3.2 Future Directions

Our results indicate that the presence of DM alters cooperativity, thus system flexibility, and affects complex formation or peptide dissociation by increasing the energetic threshold for stable binding. The next step is to determine how DM impacts the thermodynamics of peptide binding seeking confirmation for our model of DM activity. We propose to measure the thermodynamics of the peptide/MHCII (pMHCII) binding reaction in the absence and in the presence of DM, deconvoluted in enthalpic and entropic contributions, by ITC. A subset of peptides investigated by competitive binding and off-rate experiments will be selected in order to correlate changes in kinetic and binding behavior to any changes in thermodynamic mechanism of binding. The results of the thermodynamic analysis will provide an insight into how DM changes the energy of the system.

It is possible that DM will alter peptide binding by increasing the energetic threshold for stable binding through changes in the enthalpic and entropic components of pMHCII complex formation. To test this hypothesis, we will perform a thermodynamic analysis of pMHCII complexes selected on the basis of the preliminary binding and off-rate analysis. ITC will allow us to accurately measure the dissociation constant of the complexes, as well as the involved heat, which comprises the enthalpy of binding of the exothermic binding process. Entropic contribution can be easily derived by difference. On the basis of our pilot study, ITC analysis will be performed in triplicates using a DR1 protein concentrations in the calorimeter cell of ~ 5

μM and 3-fold excess DM concentrations, whereas peptide concentrations in the syringe will be $\sim 50 \mu\text{M}$. We will need to maintain a relative small concentration of DR in the cell to prevent DR aggregation, which would introduce a significant error in the measurement of the other interactions. ITC injection volume will be $2 \mu\text{l}$, and injections will be performed over 10 seconds spaced 180 seconds apart to allow for a complete return to baseline (4). Analysis of the data will yield binding enthalpy and dissociation constant. Enthalpy represents the heat energy of reaction; this term is negative when a binding interaction is formed and heat is released. The entropic contribution is a measurement of randomness of the system; this term is positive in correspondence of an increased structural flexibility of the system or upon reactants desolvation.

Since enthalpy is a state property, the calculated overall enthalpy of the ternary complex from any of the possible pathways should give identical values within experimental error. We will perform titration experiments with different protein mixtures in the calorimeter cell and the syringe to precisely identify the effect of DM on peptide/MHCII complex formation. Because DM/pMHCII binding is thought to be associated with the disruption of interactions between a specific stranded region of the MHCII alpha-chain and the peptide backbone, one could expect only the enthalpic contribution to be altered, especially if there is no significant modification of entropy between the DM-unbound and the bound state. A more likely situation is that the presence of DM prevents HLAII from providing sources of interaction to complex formation, but also decreases complex flexibility, therefore affecting both enthalpic and entropic components of free energy decrease. Either outcome will be very informative as to how peptide binding occurs in the presence of DM.

An important technical consideration is that when studying complex protein interactions by ITC, a single titration may not be sufficient to sample the shape of the binding isotherm and may not allow derivation of the binding parameters. Therefore, many titration experiments will be combined to explore the shape of the isotherm of heat as a function of three protein concentrations. SEDPHAT, software available on the NIH website, will be used to analyze the multiple ITC titration experiments and derive the thermal profiles of ternary macromolecular interactions.

Integrating the thermodynamic data with structural observations will be key to outline a comprehensive model of peptide binding to MHCII and DM activity, which will greatly support epitope prediction and development of peptide-based vaccines.

3.3 References

1. Ferrante A, Gorski J. A Peptide/MHCII conformer generated in the presence of exchange peptide is substrate for HLA-DM editing. *Nat. Sci. Rep.* 2012 Apr; 2(386).
2. Yin L, Maben ZJ, Becerra A, Stern LJ. Evaluating the role of HLA-DM in MHC Class II-peptide association reactions. *Immunology.* 2015 Jul; 195(2): 706-16.
3. Mazor R, Tai CH, Lee B, Pastan I. Poor correlation between T-cell activation assays and HLA-DR binding prediction algorithms in an immunogenic fragment of *Pseudomonas* exotoxin A. *J Immunol Methods.* 2015 Oct; 10-20.
4. Ferrante A, Templeton M, Hoffman M, Castellini MJ. The thermodynamic mechanism of peptide-MHC Class II complex formation is a determinant of susceptibility to HLA-DM. *J immunol.* 2015 Aug; 95(3): 1251-61.

Appendix A

The Thermodynamic Mechanism of Peptide-MHCII Complex Formation is a Determinant of Susceptibility to HLA-DM²

Running title: Thermodynamic-structural correlates of DM-susceptibility

Andrea Ferrante^{*}, Megan Templeton^{*,¶}, Megan Hoffman[¶], Margaret J. Castellini[‡]

^{*}Institute of Arctic Biology, University of Alaska Fairbanks, Fairbanks, AK 99775

[¶]Department of Chemistry and Biochemistry, University of Alaska Fairbanks, Fairbanks, AK 99775

[‡]Department of Veterinary Medicine, University of Alaska Fairbanks, Fairbanks, AK 99775

² Ferrante A., Templeton, M., Hoffman, M., and Castellini, M. The Thermodynamic Mechanism of Peptide-MHCII Complex Formation is a Determinant of Susceptibility to HLA-DM. *Journal of Immunology*. 2015 Aug; 195(3): 1251-61.

Abstract

Peptides bind Class II Major Histocompatibility Complex molecules (MHCII) through a thermodynamically non-additive process consequent to the flexibility of the reactants. Currently, how the specific outcome of this binding process effects the ensuing epitope selection needs resolution. Calorimetric assessment of binding thermodynamics for HA₃₀₆₋₃₁₉ peptide variants to the human MHCII HLA-DR1 (DR1) and a mutant DR1 reveals that peptide/DR1 complexes can be formed with different enthalpic and entropic contributions. Complexes formed with a smaller entropic penalty feature circular dichroism spectra consistent with a non-compact form, and molecular dynamics simulation shows a more flexible structure. The opposite binding mode, compact and less flexible, is associated with greater entropic penalty. These structural variations are associated with rearrangements of residues known to be involved in DM binding, affinity of DM for the complex, and complex susceptibility to DM-mediated peptide exchange. Thus, the thermodynamic mechanism of peptide binding to DR1 correlates with the structural rigidity of the complex, and DM mediates peptide exchange by “sensing” flexible complexes in which the aforementioned residues are rearranged at a higher frequency than in more rigid ones.

Introduction

MHC class II (MHCII) molecules are transmembrane heterodimeric proteins expressed on the surface of APCs and are fundamental in initiating or propagating an immune response by presenting antigenic peptides to CD4⁺ T lymphocytes. Newly synthesized MHCII molecules are transported from the endoplasmic reticulum to the MHCII compartments (MIIC) as multimeric complexes with the chaperone protein invariant chain (Ii). Ii stabilizes the nascent MHCII and prevents the binding of other peptides that are present in the endoplasmic reticulum (1). Upon arrival in the MIIC, the Ii molecule is cleaved primarily by cathepsin S (and to a lesser extent by cathepsins L, V, F and K) (2), leaving a peptide fragment termed class II-associated invariant chain peptide (CLIP) in the MHCII binding groove. For most MHCII alleles, CLIP is released by the action of the non-classical MHCII molecule HLA-DM (DM) to allow antigenic peptides to bind MHCII (3, 4). The role of DM exchange is not limited to CLIP, as it can catalyze the exchange of antigenic peptides to select for a stable peptide/MHCII (pMHCII) repertoire (5).

The crystal structures of peptide-complexed MHCII molecules have shown that peptide binding relies on interactions between pockets lining the class II groove and side chains of the peptide, and on a series of hydrogen bonds between non-polymorphic MHCII side chains and the peptide backbone (6). The primary pockets are indicated as P1, P4, P6 and P9, with P1 being the pocket located at the N-terminal side of the complex, and the individual interaction is allele-specific, due to the size and the hydrophobicity of the pocket. The encapsulation of bulky hydrophobic side chains of the peptide into the P1 pocket of the human MHCII HLA-DR (DR) is considered a requirement for stable peptide binding (7, 8), and is regarded as a major source of binding energy (9, 10).

Due to its role in the generation of the MHCII-restricted peptide repertoire and in stimulating the presentation of immunodominant epitopes, DM activity has been the focus of intense investigation. DM would function as an enzyme, facilitating the release of the peptide bound to MHCII and accelerating peptide exchange (11). However, the susceptibility to DM action varies among peptides, and significant efforts have been made to identify the features of a pMHCII complex that make it a target for DM. In keeping with a recently published review, we think that significant insights gained particularly in the last decade suggest two possible, non-mutually exclusive factors determining DM-susceptibility (12). The first model indicates that the occupancy state of the P1 pocket plays a major role in determining DM-susceptibility. For

instance, it has been shown that DM specifically binds DR2 variants in which the N-terminal site of the complex was emptied (13), and the crystal structure of a covalent DM-DR1 complex has been resolved in which the antigen was a covalently linked peptide lacking three N-terminal residues, thus leaving the P1 pocket vacant (14). The second model proposes that DM-susceptibility correlates with the pMHCII complex undergoing conformational rearrangements. In support of this model are SDS-based studies of complex stability (7, 15) and, more recently, the analysis of α F54-substituted DR1 molecules bound to a high-affinity peptide (16). This latter study showed that these mutants are more susceptible to DM-mediated peptide release than wtDR1, they feature increased affinity for DM, and increased peptide vibration, especially in the H-bonding network at the N-terminal site of the complex. The resolved structure of HLA-DO (DO) bound to DM points again to the possibility that conformational variation of the MHCII, in particular alterations in the α -subunit 3₁₀ helix and adjacent regions are responsible for tight binding to DM (17). In the same vein, we have shown that MHCII molecules loaded with different peptides sharing a Y at P1 can assume two conformations that are either susceptible or resistant to DM-mediated peptide release. The generation of the susceptible isomer appears to be correlated to the affinity of the bound peptide for DR or can be triggered by adding a second peptide to a reaction containing only the resistant form (18).

The evidence that peptides able to fill the P1 pocket are potential DM targets leaves the question open as to which complex features might be responsible for DM-susceptibility, and whether these features are somehow related to the peptide sequence. Here we show that DM-susceptibility is determined by interactions throughout the peptide binding site, in that the thermodynamic mechanism adopted by a pMHCII dyad for binding, irrespective of P1 occupancy state, is reflected in the overall conformation and residual flexibility post-complex formation. In turn, these structural features correlate with DM-mediated peptide release. This resolves the question of epitope prediction to one of predicting the structural features of the complex.

Materials and Methods

Peptide synthesis

Peptides derived from the sequence GPKYVKQNTLKLAT, representing residues 306-319 of the hemagglutinin protein from influenza A virus (H3 subtype), are described in Table A.1. The N-terminal Gly facilitated labeling. Side chains in the HA peptide are numbered relative to the P1Y residue (19). N-terminal labeling with FAM (Molecular Probes, Life Technologies Corporation) was performed on the resin before deprotection, and then peptides were cleaved and purified by HPLC and confirmed by MALDI-TOF mass spectrometry (Protein Nucleic Acid Facility, MCW).

Expression and purification of recombinant soluble DR1 protein

Recombinant soluble empty (peptide free) DR1 was produced and purified by ioGenetics (Madison, WI) from a stably transfected *CHO* mammalian cell line with a proprietary retroviral vector transduction system essentially as described for antibodies (20). The genes code for proteins of 192 (a) and 198 (b) residues, which terminate just before the beginning of the predicted transmembrane spans (residues 193-197 and 199-203 respectively). The vector was designed to generate a poly-His tag at the C-terminus of the expressed protein. DR-expressing clones were selected and expanded. His-tagged DR1 proteins were purified with a His-trap HP column coupled to an ÄKTAFPLC chromatography system, and buffer exchanged into PBS (7 mM Na⁺/K⁺ phosphate, 135 mM NaCl, pH 7.4) using centrifugal ultra-filtration (Amicon). Soluble FLAG-tagged DM was isolated from a stably transfected *Drosophila S2* cell line as described (21). To avoid contamination with FLAG peptide, DM elution from the resin was performed with 0.1 M glycine HCl, pH 3.5. Both DR1 and DM proteins were purified and buffer exchanged into K/Na-phosphate buffer (1.47 mM KH₂PO₄, 8.1 mM Na₂HPO₄, 135 mM NaCl, 2.7 mM KCl, pH 7.4) using centrifugal ultra-filtration (Amicon). Purity (>95%) was confirmed by SDS-PAGE stained with GelCode Blue Stain Reagent (Pierce). DR1 proteins were quantified by measuring the UV absorbance @ 280 nm using an E₂₈₀ of 45,494 M⁻¹ cm⁻¹ before use as calculated with the Expasy ProtParam tool (54).

Generation and expression of β 81-mutated DR1 molecules

Plasmids encoding truncated forms of the HLA-DR α and DR β *(0101) genes were the gift of Dr. Lawrence Stern (U. Mass. Medical School) (22). Position 81 His of the β chain was mutated to Asn through the use of the QuikChange site-directed mutagenesis kit (Stratagene) and the primer 5':CCAACCCCGTAGTTGTTTCTGCAGTAGGTGTC:3'. The mutation was confirmed by sequencing, and wt α and mutant β plasmids were cotransfected into CHO cells for subsequent production by ioGenetics as indicated above. SDS-PAGE analysis of purified β 81mut and DR1 proteins revealed no significant differences in migration or purity.

Isothermal titration calorimetry (ITC)

Titration calorimetry was carried out with a Microcal ITC200 (GE Healthcare). Analysis was performed at least in triplicate with peptide in the syringe and DR1 in the calorimeter cell at 25 °C, pH 7.4. Starting protein concentration in the calorimeter cell was 5 μ M, whereas peptide concentration in the syringe was 50 μ M. ITC injection volumes were 2 μ l, and injections were performed over 10 s at a steering speed of 500 rpm spaced 180 s apart to allow for a complete return to baseline. Dilution heats were measured by titrating 50 μ M of peptide from the syringe into the cell containing only buffer. Data were processed and integrated with Origin software. Single data sets were fit to a single site ITC binding model, using a baseline offset parameter to account for heat of dilution. The first data point was excluded from analysis due to dilution across the injection needle tip.

Peptide/MHCII (pMHCII) complex generation

pMHCII complexes were formed by incubating 1 *m*M MHCII protein with a 10-fold molar excess of either unlabeled or FAM-labeled peptide (depending on the experiment) in PBS (pH 7.4) and protease inhibitors for 16-18 h @ 37 °C. pMHCII complexes were then purified from unbound peptide with a Centricon-30 spin filter that had been pre-incubated with 25 mM MES (pH 6.4). Purified complexes were then quantified by reading the UV absorbance @ 280 nm, factoring in an E_{280} of 1280 $M^{-1} cm^{-1}$ for the Y residue and 10846 $M^{-1} cm^{-1}$ for the fluorescein present in the bound peptide. The latter measurements would add to the extinction coefficient endogenous value reported above.

Circular dichroism spectroscopy (CD)

For CD analysis, empty and peptide-loaded complexes were exchanged into 5 mM sodium phosphate/5 mM sodium acetate buffer, pH-adjusted with concentrated stocks of HCl and filtered to a final concentration of 3.5 μ M (~0.2 mg/ml). Dichroism measurements were made using a 1-mm path length cuvette on a Jasco J-720 spectrophotometer. Wavelength scans were obtained using 1.5-nm bandwidth, constant 10 °C temperature, and 1-nm sampling with a 5-second dwell time per point. All experimental scans were adjusted for background signal by subtracting out the signal from a dialyzing buffer scan.

Thermal denaturation

Thermal stability data was obtained by monitoring the CD signal at 204 nm while the temperature was increased from 10 °C to 90 °C, using 1 °C intervals, 1-minute equilibration time, 1-minute dwell time at each temperature, and 2-nm bandwidth. For each unfolding transition, the midpoint temperature T_m was determined as a peak in the first derivative function of the unfolding curve, and also separately by curve-fitting to a seven-parameter function that describes a two-state transition (23, 24):

$$\theta = (\theta_u + m_u T) + \left[\frac{(\theta_f - \theta_u) + T(m_f - m_u)}{1 + e^{\left[\frac{\Delta H}{RT} + \frac{\Delta C_p}{R} \left(\frac{T_m}{T} - 1 + \ln \frac{T}{T_m} \right) \right]}} \right]$$

where θ_u and m_u describe the slope and y-intercept of the unfolded state baseline; θ_f and m_f describe the slope and y-intercept of the folded state baseline; T_m is the midpoint of the transition (where $\Delta G = 0$); ΔC_p is the heat capacity change upon unfolding; and ΔH is the enthalpy of unfolding at the T_m . The thermodynamic values derived in this analysis are likely to depend on the concentration at which the equilibrium is measured, and therefore only holds for the concentration ranges tested (0.1–1 mg/ml) (24). The relationship of the unfolding transition to an irreversible denaturation that occurs in the same temperature range was investigated by recording the dependence of the midpoint temperature on the rate of the scan for overall scan rates 0.33 °C/min to 1.33 °C/min. As described previously for DR1, only a slight dependence was observed over the rates tested, indicating that the two-state approximation can be used at the experimental scan speeds (8, 25).

Molecular dynamics (MD) simulation

The MD simulation was performed with the software package NAMD (26) using the CHARMM22 force field with an explicit water model and all simulations were carried out at constant temperature (298 K), pressure (1 atm). All molecular graphics images were generated using the Visual Molecular Dynamics (VMD) software (27). The structure of the MHC class II molecule in complex with peptide epitope (PDB: 1DLH) was taken from the Protein Data Bank. The complexes formed by HA-substituted peptides and DR1 or β 81mut were prepared by applying the appropriate mutations within the sequence of the wt peptide with the VMD mutator plugin, version 1.3.

The peptide/MHC complex was solvated in a box of transferable intermolecular potential (TIP) water with at least 10 Å distance between protein and the boundary of the water box. The system was first minimized with 10,000 steps of steepest descent followed by 100,000 steps of conjugate gradient descent. The MD simulation time step was 2 fs, and trajectory was saved every 1 ps. The length of the simulation was determined by monitoring the convergence of various mechanical properties of the system. The simulation was stopped when the value for the RMSD did not fluctuate more than 3.0 from its average value during 2 ns. As previously indicated, when the simulation reaches an RMSD that oscillates around a constant value, it can be assumed the system has converged to a stable or a metastable structure. A twin range cut-off of 0.9/1.4 nm for van der Waals interactions was applied, and the particle mesh Ewald method was used to treat long-range electrostatic interactions. Constant temperature was controlled by Langevin dynamics, and pressure was maintained by using Nosé-Hoover Langevin piston pressure control.

Surface plasmon resonance (SPR)

SPR experiments were performed on a Biacore 2000 instrument. Anti-FLAG antibody M2 for DM capture was immobilized on the CM5 sensor chip using standard amine coupling procedure. FLAG-tagged DM was diluted to 75 µg/ml in 10 mM Sodium Acetate. 5000 RU of DM protein were immobilized on the anti-FLAG coated chip at a flow rate of 5-10 µl/min at 25 °C, and the surface was subsequently blocked with 1M 2-aminoethyl-sulfate and washed with 50 mM CAPS solution. Affinity experiments were performed by injecting the various pMHCII complexes in two fold dilutions and at seven concentrations from 8 mM and run over the DM surface at flow

rate of 5 $\mu\text{l}/\text{min}$. The running buffer in all phases was composed of 10 mM sodium citrate pH 5.5, 150 mM NaCl, 3 mM EDTA, and 0.05% (vol/vol) surfactant P20. PBS buffer, 0.05% (vol/vol) surfactant P20 was used for control experiments at pH 7.4. Regeneration of the DM-coupled surface was carried out by flowing 50 mM CAPS pH 11.5 for 30 s until a stable baseline was reached. Binding data were fit to a Langmuir binding model using BIAeval software.

Fluorescence polarization (FP) dissociation measurements

Intrinsic and DM-mediated peptide dissociation measurements were performed via FP, which quantifies the ratio between bound and free fluorophore-labeled ligand by measuring the tumbling speed of the fluorophore, as the speed is faster when the ligand is unbound. 100 nM of purified complexes generated as indicated above were incubated with 100-fold excess of unlabeled HA₃₀₆₋₃₁₉ peptide and 3-fold excess DM where required. In past analysis we have shown that, in our system, a DM/complex ratio < 3 is not sufficient to promote peptide exchange. It was also reported that in the MIIC, the DM:MHCII ratio is 1:5 (28). Our observations might be affected by the 3D geometry of reaction, with respect to the planar situation of membrane-bound MHCII molecules; nevertheless the majority of published data relative to DM activity have been collected by using soluble DM in kinetic experiments. Reactions were performed at 37 °C in 50 mM sodium citrate/sodium phosphate buffer at pH 5.4 and were covered with mineral oil to prevent evaporation. To avoid non-specific adherence of the protein, treated black polystyrene 96-well plates were used (Corning), as indicated in ref. (29) and (33). Measurements were performed using a Wallac VICTOR counter (PerkinElmer Wallac) with the excitation $\lambda = 485$ nm and emission $\lambda = 535$ nm. Specific control groups included (a) protein only, (b) peptide only, and (c) buffer only, and were used for background correction. FP values were transformed in fraction of bound peptide with the equation: $P_{\text{bound}} = \frac{FP_x - FP_{\text{free}}}{FP_{\text{bound}} - FP_{\text{free}}}$, where FP_x indicates the value of FP measured by the counter at $t = x$ (minutes), FP_{free} indicates the value of FP relative to free peptide, and FP_{bound} indicates the value of fluorescence polarization of the complex. We assume that the latter value coincides with the value of FP measured at $t = 0$ of the experiment, since we have shown that we are able to isolate pMHCII complexes with a bound MHCII/total MHCII ratio $\geq 90\%$ and bound peptide/total peptide $\geq 97\%$ (33). Fraction of bound peptide is then plotted against time and fit to a one- or a two-phase exponential function for $t_{1/2}$ calculation. Each

experiment was performed in triplicate, and the reported dissociation rate reflects the mean \pm SD of three independent experiment

Results

Peptide-MHCII dyads form complexes with different thermodynamic mechanisms.

In our past investigation of peptide binding to and release from MHCII we have observed by indirect approaches the occurrence of isothermal entropy-enthalpy compensation (iEEC) (30) and binding cooperativity (30-32), and we interpreted them as the thermodynamic epiphenomena of the system structural flexibility. Those experiments were performed with a panel of peptides derived from the sequence of HA₃₀₆₋₃₁₉ via cycle mutation, and HLA-DR1 (DR1) or a mutant DR1 (β 81mut), in which formation of the H-bond between the peptide backbone and the non-polymorphic His at position 81 of the β -chain (β 81 H-bond) is inhibited by a H^N mutation. Among those sequences we identified a peptide, HASG, in which the combined effect of the P2V^S and P10A^G mutations resulted in a ~4 fold decrease of K_D for DR1 as assessed in competitive binding assays (32, 33). Though HASG can still be considered a high-affinity binder, its intrinsic kinetic stability for DR1 and β 81mut was found to be significantly decreased with respect to the wt sequence. Thus, we reasoned that this sequence would be particularly suitable to investigate the potential association among thermodynamic mechanism adopted for binding, structural conformation of the resulting complex, and susceptibility to DM action.

The thermodynamic parameters of the peptide binding reactions to DR1 and β 81mut were derived by Isothermal Titration Calorimetry (ITC). The calorimetric isotherm of binding of peptide to MHCII illustrates an exothermic binding characteristic at 25 °C. The standard enthalpy change (ΔH°), dissociation constant (K_D), and stoichiometry (n) and the standard error for each variable were derived on the basis of the one-site model fit of the peptide/MHCII complex (pMHCII) isotherm (Figure A.1). The ΔH° , K_D , and n values of peptide binding listed in Table A.1 are the error-weighted mean values and the standard error of the mean for each variable from three repeated experiments. The standard errors of the mean for standard free energy decrease (ΔG°) and standard entropy change ($T\Delta S^\circ$) were calculated using the standard error of the mean of the association constant (K_A) and ΔH° by statistical error propagation method. Observed enthalpies derive largely as a consequence of changes in interatomic interactions (e.g., hydrogen bonds, van der Waals interactions, p-p interactions), in which the sign indicates that there is a net favorable (negative ΔH) redistribution of the network of interactions between the reacting species (including solvent). Hydrophobic interactions are related to the relative degrees of disorder in the free and bound systems and thus these interactions are reflected in the entropy change. The

release of “bound” water molecules from the binding groove surface and the peptide to the bulk solvent is a source of favorable entropy (positive ΔS). A reduction in conformational states in either ligand or protein upon binary complex formation is entropically unfavorable (negative ΔS). All binding reactions are enthalpy-driven, however the measured overall entropic contribution differs, indicating that the restriction in conformational mobility occurring upon ligand binding varies as a function of the peptide. Indeed, in the case of HASG, binding to DR1 is associated with a smaller entropic penalty as compared to HA, suggesting a more pronounced residual conformational mobility post-complex formation.

The analysis of b81mut binding is consistent with our observations derived with indirect methods (30). In the case of HA, the enthalpic contribution to binding free energy does not change significantly with the b81 H-bond disruption, whereas the entropic penalty is reduced with the consequence that binding to b81mut is favored as compared to DR1. Conversely, the inability to form the b81 H-bond for HASG has a greater impact on binding free energy, in that it cooperatively prevents formation of other interactions, with a significant reduction of the enthalpic component. For this latter complex, the entropic contribution is positive, indicating that reduction in conformational mobility upon binding is limited and it reflects predominantly a favorable desolvation-related entropy change.

These results show that formation of high-affinity (pMHCII) complexes (such as HA/DR1 and HASG/DR1) can be achieved with different enthalpic and entropic contributions, and they confirm that the impact of one specific interaction on binding (such as the b81 H-bond) depends on the overall energetics of the system.

Thermodynamics of pMHCII complex formation is associated with complex secondary structure.

To investigate if alterations in MHCII secondary structure accompany the different thermodynamic profile of the various complexes, we used far-UV circular dichroism (CD) spectroscopy to probe conformational specificities of HA, and HASG bound to DR1 or the b81mut (Figure A.2 A). The CD spectrum of empty DR1 and that of empty b81mut were substantially similar to each other but altered relative to that of the HA/DR1 and HA/b81mut complexes, exhibiting decreased intensity in the positive band at short wavelengths as well as in the negative band centered at 210–220 nm. These alterations are consistent with those observed in similar investigations performed by other groups on human and murine MHCII (8, 9, 25, 34,

35). Also the spectra relative to HASG bound to either DR1 or b81mut appear similar with respect to each other, but different as compared to HA spectra, with values of ellipticity closer to the ones observed for the empty DR.

We then investigated possible differences in protein structure between the various complexes and empty MHCII by thermal denaturation measured as change in ellipticity at 204 nm (Figure A.2 B and A.2 C). Empty DR1 and b81mut featured a thermal denaturation with a midpoint temperature of the thermal unfolding transition T_m of ~ 68 °C. The presence of the peptide increased the stability of the MHCII, though this effect appears to be a function of the bound peptide and the MHCII, in that complexes featuring smaller enthalpic contributions to binding energy undergo denaturation at lower temperature (Table A.2). The slope of the θ versus temperature plot indicates a cooperative nature of denaturation. The low cooperativity of denaturation of empty MHCII suggested by the broad curve indicates that the number or strength of intramolecular contacts in this form is limited, resulting in a denaturation enthalpy ΔH_m value as low as ~ 190 kJ mol⁻¹. Cooperativity of denaturation for peptide-bound MHCII increased with respect to empty MHCII, as indicated by the steepness of the slope, and also in this case the effect appears to be a function of the peptide. To quantitate this effect we derived ΔH_m , and the difference in heat capacity ΔC_p between the folded and unfolded states. The values for ΔH_m and ΔC_p (Table A.2) indicate a global effect of peptide in stabilizing the overall folded MHC structure; however the lower enthalpy of denaturation for the multiple-substituted complexes would reflect a structurally “loose” conformation (35). These observations indicate that the thermodynamic profile of a pMHCII dyad is correlated with the conformation of the complex and its secondary structure.

MD simulation reveals greater flexibility in complexes whose formation is associated with smaller entropic penalty.

In order to assess whether differences in entropic contribution to binding energy and variation of secondary structures are correlated to differences in conformational flexibility, we performed large-scale molecular dynamics simulations of unbound MHCII molecules and MHCII bound to the peptides under scrutiny. The binding dynamics of DR1 and b81mut bound to the two peptides differed during the simulation time of 60 ns. We probed root mean square deviation (RMSD) and root mean square fluctuation (RMSF) variation between the different structures.

RMSD for all the C α atoms of the residues forming the binding site from the initial structure were calculated which was considered as the central criterion to measure the protein system. As shown in Figure A.3 A, unbound DR1 and b81mut showed deviations throughout the simulation from their respective starting structures, resulting in backbone RMSD ~ 3.2 Å for DR1 and ~ 3.3 Å for b81mut during the simulation. Complexes showed a distinct trend of deviation when compared to the unbound MHCII, in keeping with simulations performed by other groups on the same system (36-38). Interestingly, the overall RMSD fluctuations were very much similar between the HA complex bound to either DR1 (~ 1.5 Å) or b81mut (~ 1.6 Å). However, DR1 bound and b81mut bound to HASG showed more pronounced fluctuations together with a greater difference between the average RMSD values after the relaxation period (respectively ~ 2.3 Å, ~ 2.6 Å). These results suggest a greater conformational lability of the overall binding site in the case of multiple substituted complexes with altered thermodynamic profiles as compared to the HA/DR1 complex.

With the aim of determining whether the nature of the bound peptide might affect protein dynamic behavior in specific regions of the complex, the RMSF values of MHCII backbone residues were calculated for the different complexes (Figure A.3 B). Analysis of fluctuation score revealed the presence of higher degree of flexibility in DR1 or b81mut bound to HASG as compared to complexes containing HA peptide. The presence of higher RMSF values in the former structure suggests that combining the P2V"S and the P10A"G substitutions in the peptide, or breaking the b81 H-bond in the HASG/DR1 complex reduced constraints in the structural flexibility of the bound protein. The largest difference in conformational mobility can be attributed to the α -helices and to the Ig-like domains of MHCII membrane-proximal region. In particular, comparison of the average structure of the wt complex with the substituted ones indicate that, when structural shifts are visible, these involve the α -chain residues 43-54 (Figure A.3 B, arrows) as well as the β -chain residues 63-68 and 79-90 in a peptide and MHCII-dependent fashion (Figure A.3 C arrows). Such variations in flexibility, especially of the α -chain residues 43-54, a stretch of amino acids with possible involvement in DM binding, has already been described (16, 17, 37, 38).

Based on the published structure, 14 H-bonds are established between MHCII helices and the peptide backbone. In particular, residues Phe a51, and Ser a53, establish main chain-main chain interactions, whereas side chains of Asn a62, Asn a69, Arg a76, Asp b57, Trp b61, Arg

b71, His b81, Asn b82 form H-bonds with the peptide backbone. As shown in Figure A.3 D, the analysis of the overall complex H-bonding established by the aforementioned residues shows that the HA-containing complexes form more numerous and more stable H-bonds, whereas the number of H-bonds decreases in the case of complexes formed with HASG. Obviously, His b81 contribution was computed only for complexes formed by DR1, substituted by Arg in the mutated complexes. These observations are further evidence of the increase MHCII structural flexibility in multiple substituted complexes.

The graphic rendering of the MD-based structure of HASG/DR1 in comparison with HA/DR1 is shown as an example of the peptide-dependent conformation assumed by a complex, in particular at the N-terminal region (Figure A.4 A and A.4 B). The most noticeable alterations with respect to the wt complex are relative to aW43, which rotates away from the binding site and increases solvent exposure and a shift of $\sim 4\text{\AA}$ of aF51 towards the groove, resulting in a narrowing of the binding site at that end. Finally, aF54 rotates in the direction of the solvent in the substituted complex as a consequence of the inability to form an H-bond with the backbone of a more fluctuating, loosely tethered peptide. In Figure A.4 C and A.4 D the modifications in the average structures of the substituted complexes in comparison with the HA/DR1 are shown.

Taken together, these results indicate that the complexes of which formation is associated with the smallest entropic penalty, exhibit the most flexible behavior, particularly in the region that has been mapped as the DM/MHCII recognition site.

pMHCII affinity for DM and susceptibility to DM-mediated peptide exchange are determined by the thermodynamic and structural correlates of complexation.

We have shown that pMHCII dyads with comparable free energy decrease of complexation may rely on different enthalpic and entropic contributions, and a correlation can be observed between thermodynamic profile and structural features of the complex. We hypothesized that these differences in energetics and structure across complexes may impact DM-susceptibility, particularly as a consequence of the different availability of residues within the N-terminal region to interact with DM. To test this possibility, we measured the affinity of DM to the various complexes by a surface plasmon resonance (SPR) binding assay (Figure A.5). Specific saturable, dose-dependent binding was observed for HASG bound to either MHCII molecules, whereas no DM binding could be measured for the HA peptide bound to either DR1 or b81mut.

Equilibrium binding analysis revealed K_D values ~ 1.5 mM. To ensure that the binding was specific we performed these experiments at pH 7.4 and pH 5.4. The significant reduction in binding at pH 7.4 is consistent with the known pH effect on DM activity (Supplemental Figure A.1); moreover, no binding could be observed for empty DR1 and b81mut. These results clearly indicate that the complexes of which formation is correlated to a smaller entropic penalty and potentially featuring an increased structural flexibility, are preferential ligands for DM.

Finally, to investigate whether the differences in DM-affinity correlate with differences in DM activity, we measured the release of FAM-labeled peptides in the presence and in the absence of 3 fold excess DM from DR1 (Figure A.6 A) and b81mut (Figure A.6 B) via fluorescence polarization. DM-susceptibility was calculated as $k_{\text{off}}\text{-fold increase} = k_{\text{off[DM+]}}/k_{\text{off[DM-]}}$. We correlated DM-susceptibility with the restraint of conformational flexibility associated with complex formation (TDS/DG). As shown in Figure A.6 C, an exponential relationship between residual entropy and DM-susceptibility can be determined: complexes with limited conformational flexibility (right side of the plot) are the most stable in the presence of DM, whereas complexes with greater residual entropy are more susceptible to DM activity.

Taken together, these results indicate that the thermodynamic signature of a given pMHCII complex is correlated to the probability for that complex to assume a conformation targetable by DM and, as a consequence, it also determines complex susceptibility to DM activity.

Discussion

Recent structural studies have provided important insights into how DM interacts with MHCII to mediate peptide exchange (14, 16, 17). From these structures and the most recent biophysical/biochemical analyses it would appear that DM-susceptibility of a pMHCII complex is a function of the frequency with which the P1 pocket is emptied or the probability for the complex to assume a conformation in which critical residues are available for interaction with DM. However, it is still unclear which of these properties is a determinant of DM-susceptibility, and whether they are related to the sequence of the bound peptide. Conformational analysis for just a few pMHCII complexes have been carried out, limiting our capacity to infer general rules of DM-susceptibility on the basis of the nature of the peptide and structural determinants. Moreover, we still do not have a conclusive understanding of DM action on the complex and how it skews the binding of peptides.

In this work we show that the thermodynamic mechanisms adopted by peptides and MHCII molecules to interact may be different, as defined through the enthalpic and entropic components of binding free energy decrease, even in the case of peptides with comparable affinity for the same MHCII. Whereas these energy variations maintain an enthalpy-based mechanism of complex formation, CD and MD simulation indicate that they are sufficient to affect the conformation and the lability of the resulting complex. SPR and FP-based analyses reveal that these conformational differences are correlated with the affinity of the complex for DM and its susceptibility to DM-mediated peptide exchange.

Peptide binding in the absence of DM is a flexible process, and does not rely on independent contributions from pocket/anchor interactions and H-bonds, but is a function of the synergism involving multiple single-point interactions (30, 31, 39). MHCII molecules feature conformational lability, and the α -subunit 3₁₀ helical region with the adjacent extended strand, the β 2 Ig-like domain, and the pronounced kink in the β -subunit helical region β 62-71 are the most subject to conformational heterogeneity, either in the empty or in the bound state (40). We have previously shown that the effect of MHCII flexibility on the transition from the empty to the bound state (and vice versa) is evidenced by phenomena such as cooperativity and isothermal entropy-enthalpy compensation, the latter also confirmed in the present work (30). These observations suggest a thermodynamic-structural model by which peptides and MHCII bind by optimizing the available interactions through search of conformational space and, as they bind,

system flexibility is restrained; the relative enthalpic and entropic contributions to binding free energy decrease determines the structure and conformational lability of the resulting complex.

How does the overall binding property of the peptide determine DM-susceptibility of the complex? The correlation between thermodynamic mechanism of binding and complex structure strongly suggests that the interplay between entropy, enthalpy and binding cooperativity are responsible for determining the probability by which a complex is generated and assumes a more or less DM-susceptible conformation. Indeed, the CD and MD analyses show that a complex, of which formation is correlated to a smaller entropic penalty, features greater conformational mobility and a secondary structure closer to the empty MHCII form as compared to an isoenergetic complex of which formation involves a larger enthalpic contribution. As a consequence, regions within the N-terminal side of the former complexes are expected to disengage from interactions with the peptide and be more amenable to interaction with DM at a higher frequency than the latter.

Studies performed with peptides unable to fill the P1 pocket have suggested a model by which DM-susceptibility is a function of the interactions at the P1 region (9, 13, 15, 41, 42). This model has been further refined by a recent structure of DM-DR1 complex with DR1 covalently linked to a peptide lacking three N-terminal residues (14). According to this latter study, suboptimal P1 anchor residues would favor formation of a complex in which the peptide N-terminal dissociates from MHCII, and residues α W43, α F51 and β F89 would rotate out of the pocket, consequently becoming available for DM binding and not accessible to interactions with the peptide. The destabilized complex bound to DM would be able to exchange peptides and DM would dissociate from DR1 once the latter is bound to a peptide able to fill the P1 pocket and possibly capable of forming interactions at the other three major pockets. However, this model does not fully account for the observations that even peptides with optimal “anchor” residues are DM-susceptible when bound to MHCII (43, 44). In a similar fashion, this same model is not able to explain the evidence that such peptides are unsuccessful in replacing completely a DM-sensitive ligand such as CLIP during a DM-mediated peptide exchange reaction (33). The alternative classical hypothesis of DM-susceptibility based on disruption of one or multiple H-bonds, especially the one established between the His at b81 of the MHCII and the peptide backbone (45, 46) has been challenged by several studies in which complexes lacking one or more of these same H-bonds appeared to be more susceptible to DM than their wild-type

counterparts (47-49). We have previously shown that the disruption of the b81 H-bond affects peptide binding and complex kinetic stability differently on the basis of overall energetics of the complex (30, 32). Our current analysis indicates that also the effect of the b81 H-bond on DM-susceptibility varies across complexes, of which conformation and lability differ, as determined by the thermodynamic mechanism of binding.

The model we suggest can explain and reconcile all these conflicting observations: structural studies have mapped the DM/MHCII recognition site to the extended strand loop of the alpha chain (14, 16, 50, 51), which is also one of the most dynamic regions of the complex (40). The occupancy state of the P1 pocket region ought to be one important determinant of the geometry of the DM/DR interface. However, due to cooperative effects, stable encapsulation of peptide side chains in the P1 pocket and concurrent formation of the H-bond network at the N-terminal side of the complex relies on interactions formed at other positions of the groove, including the C-terminal side. Indeed, a peptide featuring a suboptimal or poor P1 anchor, such as A for HA/DR1, not stabilized by other interactions across the groove, will be sufficient to promote those structural rearrangements leading to a DM-susceptible form of the complex. However, it would be theoretically possible to rescue suboptimal P1 anchors from causing DM-susceptibility by modifying interactions at other positions of the peptide. For instance, we are currently examining the combined effect of the P1N substitution, which is significantly destabilizing in the context of HA peptides, with P4E and P7G, which appear to increase stability of the peptide in a DM-mediated exchange reaction. In the same vein, the role of the b81 H-bond and of any other H-bond in favoring the conformational rearrangement required for DM-susceptibility are a function of the overall binding energy and conformational flexibility of the system. Indeed, DM-susceptibility of HASG is increased by the b81 mutation, whereas HA is barely affected. We can also propose an explanation as to why the complex formed by a P1A-substituted HA peptide with the b81mut does not behave differently in terms of DM-susceptibility as compared to a complex involving the wtMHCII: since the emptied P1 pocket, not sufficiently stabilized by other interactions across the binding groove, is already rearranged in the DM-susceptible form, the contribution to this rearrangement of the b81 H-bond loss is expected to be minimal (45). In addition to the effect of multiple interactions across the groove on the binding state of the peptide at the P1 pocket region, there is also a direct effect of each position on the conformation of the complex. Finally, the thermodynamic mechanism adopted by

the system will determine the residual flexibility post-complexation, hence the probability for the DM/DR interaction site to assume a conformation amenable to DM binding. Thus, we can define a spectrum of DM-susceptibility in which one extreme is represented by complexes with reduced conformational mobility, fully occupied P1 pocket region (such is the case of HA₃₀₆₋₃₁₉ bound to DR1), or suboptimally occupied but stabilized, that do not bind DM and are not amenable to DM-mediated exchange. The opposite extreme would be represented by complexes of which structure and lability would permit DM interaction, but of which limited intrinsic stability cannot be further reduced by DM action, such as “anchorless” HA₃₀₆₋₃₁₉. Between these two extremes are included all those pMHCII systems that can form a complex, of which overall structure and flexibility determined by respective binding thermodynamics define DM-affinity and susceptibility.

Two aspects of the present study pose a limit to the generalization of our conclusions. First, this analysis is limited to four, closely related DR/HA variant complexes, and it might be argued that the identified thermodynamic correlates of DM susceptibility are valid only in such instances where limited structural changes are applied to the system. This consideration should necessarily be taken into account if we attempted to derive rules of DM-susceptibility on a peptide-sequence basis. Extending this study to a larger number of complexes formed by different MHC alleles and different peptides will help reach that goal. Nevertheless, this argument does not invalidate the correlation between thermodynamic mechanism of binding and DM-susceptibility, irrespective of the structural features of the peptide, since the analyzed thermal parameters are state functions. Moreover, this argument would not nullify our observation that peptides able to fill the P1 pocket can be DM-susceptible, which is a clear evidence against a P1-centric model of DM function.

The second limitation is that the DM dissociation experiments are correlative, and although supportive, the molecular dynamic simulation studies are not conclusive as to the structure of the conformers and the molecular aspects of the complex associated to DM activity. EPR and NMR-based experiments are underway to determine the structure of the conformers and mechanisms of DM interaction. Interestingly, our findings are consistent with a recent structural (and kinetic) study showing that DM-susceptibility would be determined by a dynamic MHCII conformation, and indicating the modifications the complex undergoes as it switches from a DM-resistant to a

DM-susceptible form (52). We expect to identify similar conformational rearrangements in our system by structural analysis.

The initial observations relative to DM activity indicating a role in facilitating CLIP release from MHCII have determined the adoption of kinetics-based approaches to the study of DM-susceptibility (3, 21, 53-55). However, the conclusions reached from these experiments have been controversial, and they are not easily applicable to the problem of epitope selection in the context of the APC. The panoply of peptides generated by endocytosed proteins includes a consistent number of ligands with low affinity for a given MHC allele, sequences with intermediate affinity and few high-affinity ones. At the end of epitope selection in DM-competent cells, MHCII molecules reach a thermodynamic equilibrium in which they are complexed with stable, high affinity binders. It is difficult to explain how the MHC-peptide system may reach such equilibrium intrinsically in consideration of the evidence that the transit time of an MHCII through the MIIC is comparable to the dissociation rate of many low-intermediate affinity peptides (56). Indeed, if this were the case, the expectation would be that the majority of MHC molecules are bound to low- or intermediate-affinity peptides that are in excess, as a consequence of a kinetic control of the selection process. We prefer the possibility that epitope selection is regulated by a mechanism able to enhance the thermodynamic control of the peptide binding process, with DM the likeliest factor determining the thermodynamic equilibrium of the endosomal machinery. This possibility is supported by the evidence that DM deficient APCs present a significant amount of empty MHCII or MHCII bound to low-affinity peptides (55, 57). Our observations are a further confirmation of the correlation between thermodynamic signature of a pMHCII complex, its conformational flexibility, and susceptibility to DM-mediated peptide exchange. Thus, in conjunction with the published structural studies, our work provides a comprehensive theory to explain peptide binding and DM activity within the timeframe allotted for epitope selection.

Acknowledgements

We thank Dr. Jack Gorski for providing reagents and for critically reading and reviewing the manuscript, ioGenetics for providing DR1 and β 81mut proteins, Dr. Lawrence Stern (UMASS) for β 81mut constructs, Dr. Dennis Zaller (Merck & Co.) for DM expressing S2 cells, Trudy Holyst (BCW) for peptide synthesis.

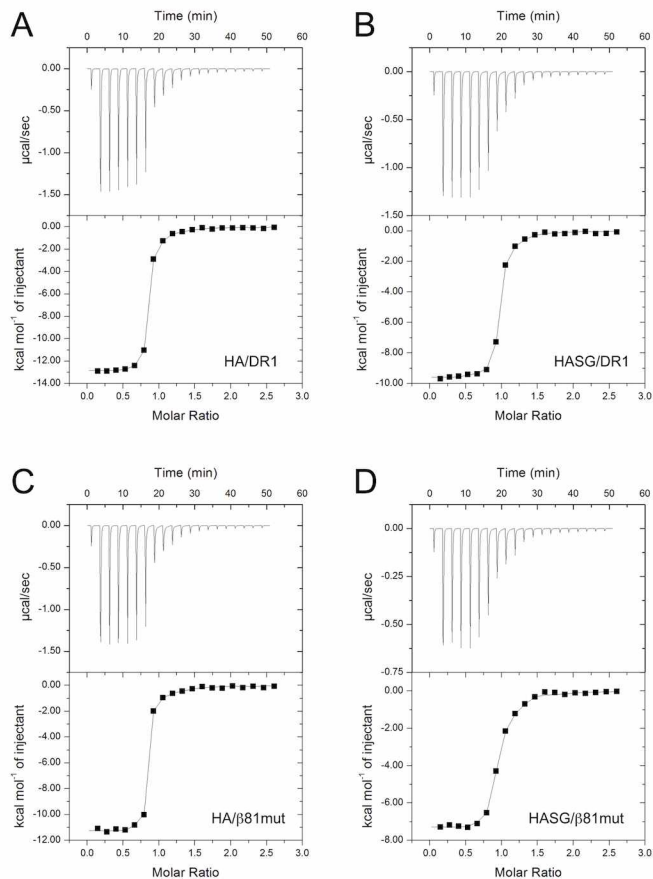


Figure A.1 – Representative Raw ITC Data Titrating HA-derived Peptides into HLA-DR1 and β 81mut and the Fitted Binding Curves. Starting protein concentrations in the calorimeter cell was $\sim 5 \mu\text{M}$, whereas concentrations in the syringe was $\sim 50 \mu\text{M}$. ITC injection volumes were $2 \mu\text{l}$, and injections were performed over 10 s spaced 180 s apart to allow for a complete return to baseline. Data were processed and integrated with Origin software. Single data sets were fit to a single site ITC binding model, using a baseline offset parameter to account for heat of dilution. The first data point was excluded from analysis due to dilution across the injection needle tip. Experiments were performed at least in triplicate. Measured thermal parameters are indicated in Table A.1.

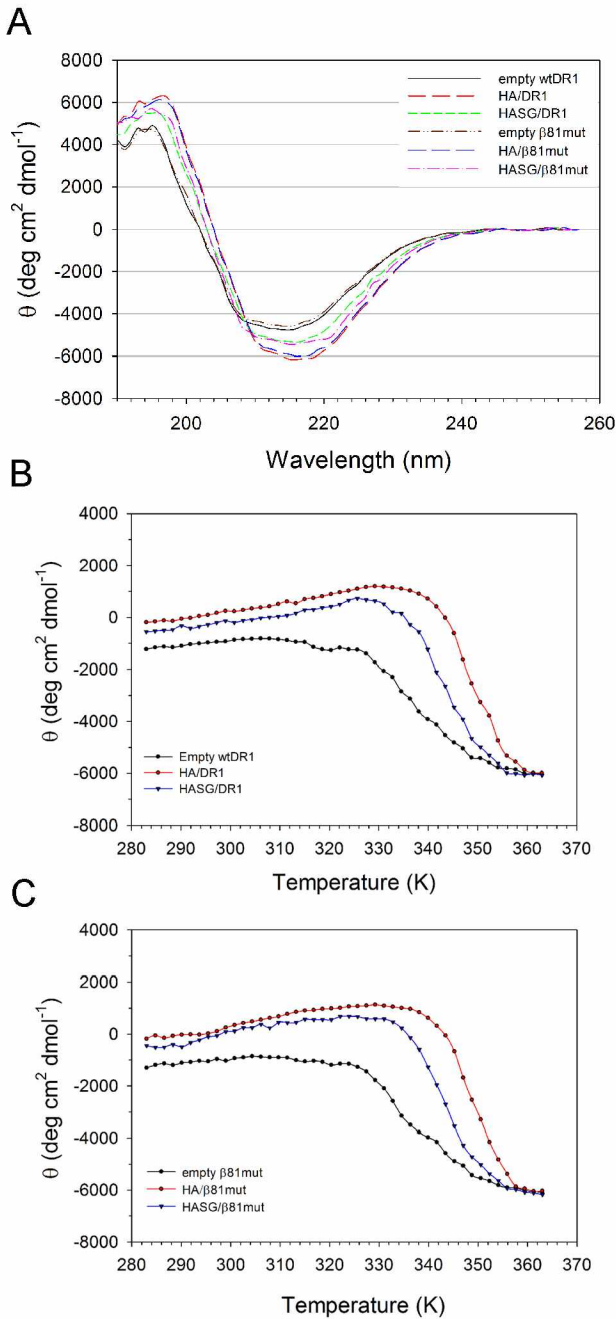


Figure A.2 – Far-UV CD and Thermal Stability Analysis of Empty MHCII Molecules and Different pMHCII

Complexes. (A) Changes in secondary structure of empty MHCII molecules and molecules bound to either HA or HASG. **(B, C)** Thermal denaturation curves of empty MHCII (black line) and MHCII bound to HA (red line), HASG (blue line) are shown for reactions involving DR1 **(B)** and β 81mut **(C)**. Spectra were acquired on a Jasco J-720. Complexes were exchanged into 5 mM sodium phosphate/5 mM sodium acetate buffer, pH-adjusted with concentrated stocks of HCl and filtered to a final concentration of 3.5 μ M (~0.2 mg/ml). For the thermal stability analysis, temperature was increased by 1.0 K min⁻¹. The extent of thermal denaturation was measured as a change in ellipticity at 204 nm. Thermodynamic parameters derived as described in Methods are reported in Table A.2.

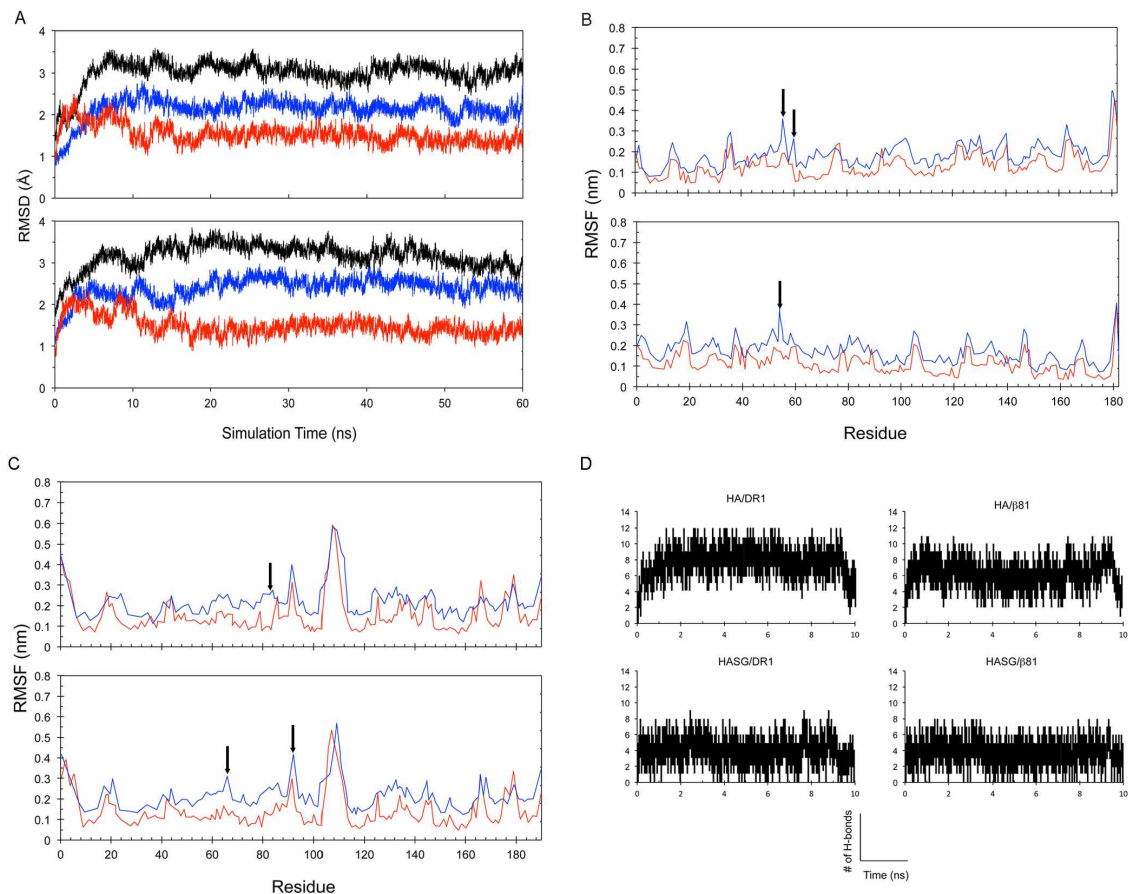


Figure A.3 - MD Simulation of Empty MHCII and MHCII Bound to Different Peptides. The starting conformation was extracted from PDB 1DLH. The complexes formed by HA-substituted peptides or by $\beta 81$ mut were prepared by applying the appropriate mutations within the sequence of the wt peptide or DR1 with the VMD mutator plugin. **(A)** RMS deviation over time for the peptide-loaded (red: HA, blue: HASG) and free (black) simulations, for the DR1 **(top)** and $\beta 81$ mut **(bottom)** $\alpha 1$ $\beta 1$ binding site. **(B, C)** RMS fluctuation during the first 10 ns of simulation for each residue (all atoms included) for the α -subunit **(B)** or β -subunit **(C)** of the DR1 **(top)** or $\beta 81$ mut **(bottom)** complexes. Color code as in panel A. **(D)** H-bonding between MHCII helices and peptide backbone for the four complexes is shown during the first ten ns of simulation.

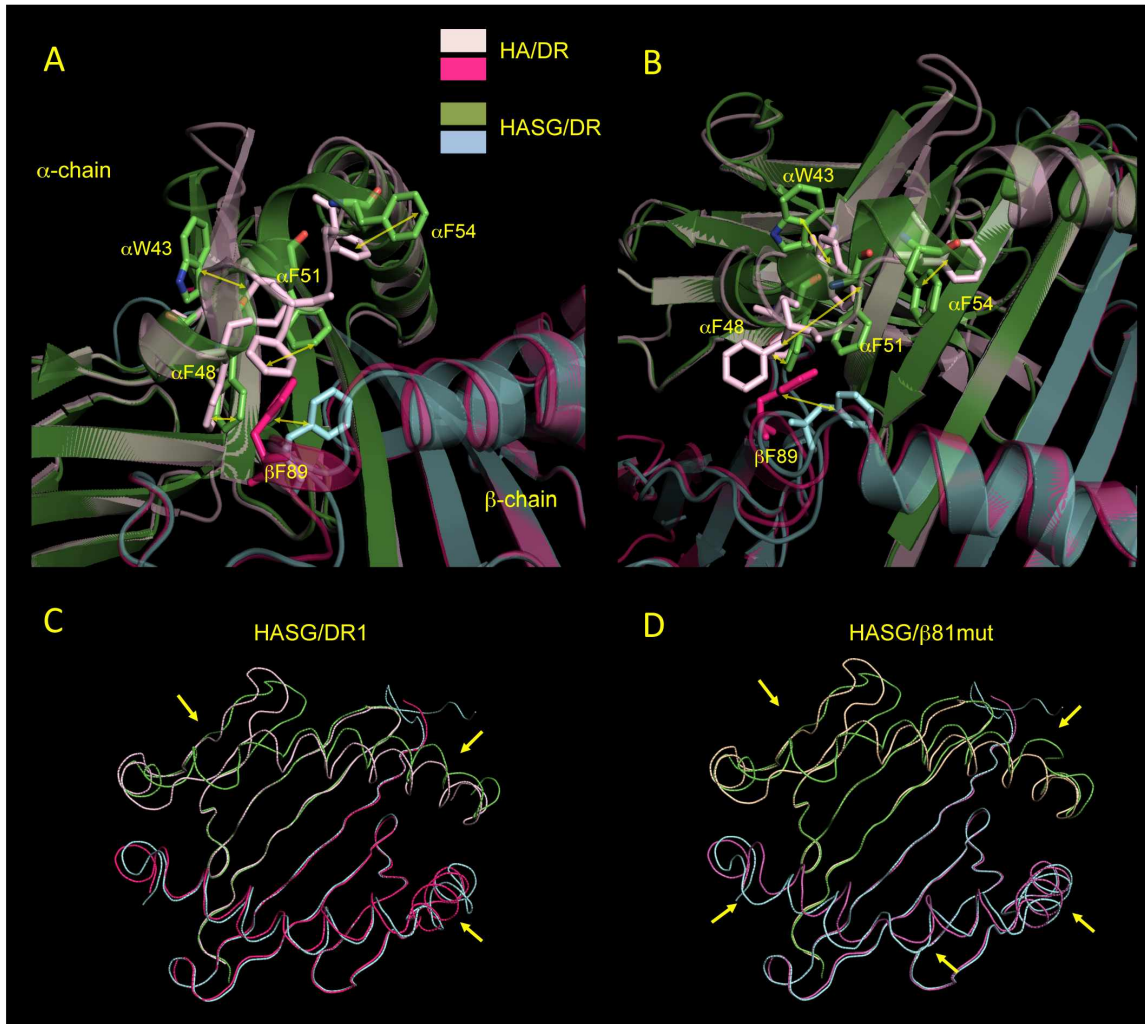


Figure A.4 – Structural Model of Peptide-dependent pMHCII Complex Modifications. In the top panels, the most favored conformers of the HASG/DR1 and HA/DR1 complexes are shown superimposed at the N-terminal region from the side (**A**) and from the top (**B**). Residues postulated to be involved in DM interaction are shown as sticks, and predicted conformational rearrangements are indicated. In the bottom panels, the most favored conformers of the HASG/DR1 (**C**), and HASG/b81mut (**D**) complexes are shown superimposed with HA/DR1 complex. Regions undergoing the most pronounced conformational rearrangements are indicated. In all panels the wt complex is rendered in light pink (a-chain) and magenta (b-chain). The substitute complex is shown in green and cyan. The peptide is not shown in these renderings for graphic clarity.

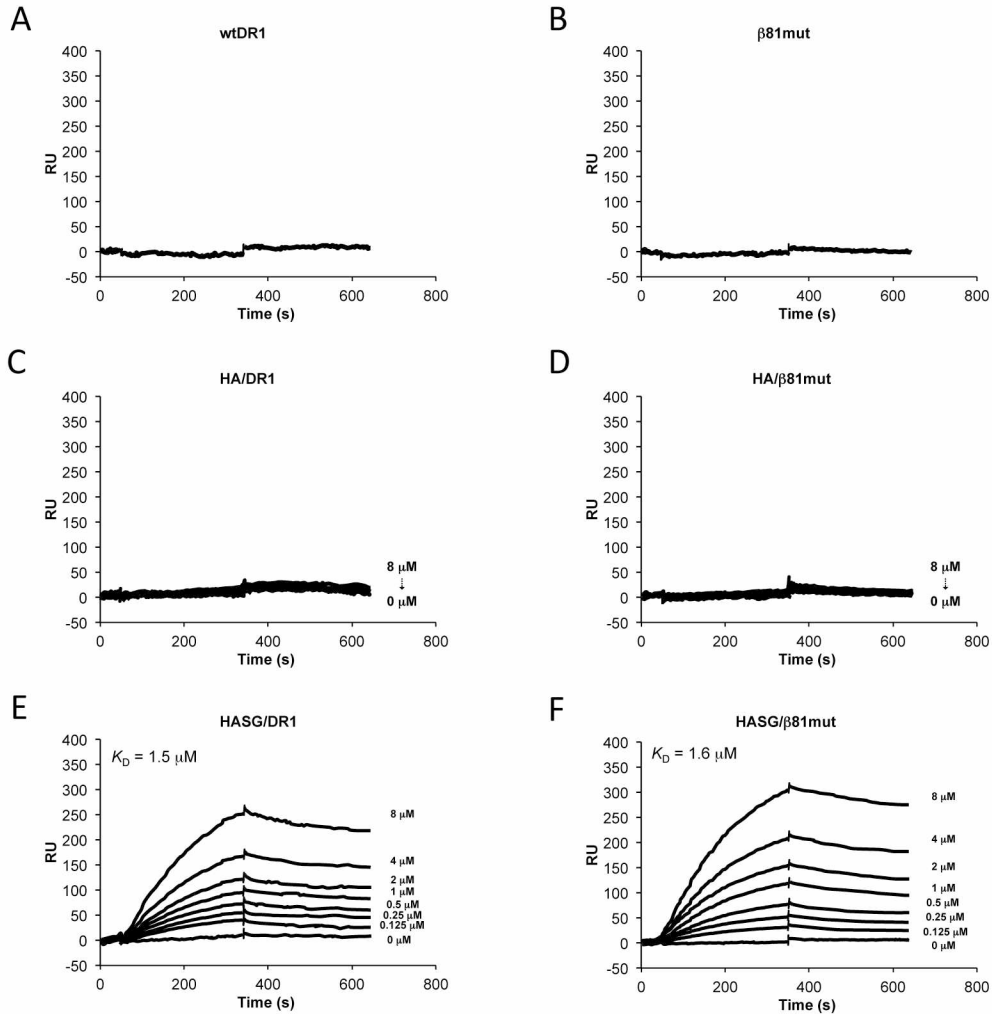


Figure A.5 - SPR Assay of DM Interaction with pMHCII Complexes. Affinity measurements were performed by injecting the various pMHCII complexes or empty MHCII molecules in two fold dilutions and at seven concentrations from 8 mM and flowing them over DM-coated CM5 sensor chip at flow rate of 5 μ l/min for 5 min and dissociated for 5 min. Binding to DM was analyzed for (A) unbound DR1, (B) unbound b81mut, (C) HA/DR1, (D) HA/b81mut, (E) HASG/DR1, (F) HASG/b81mut. These experiments were repeated at least three times. Binding data were fit to a heterologous binding model using BIAeval software to derive the indicated K_D values.

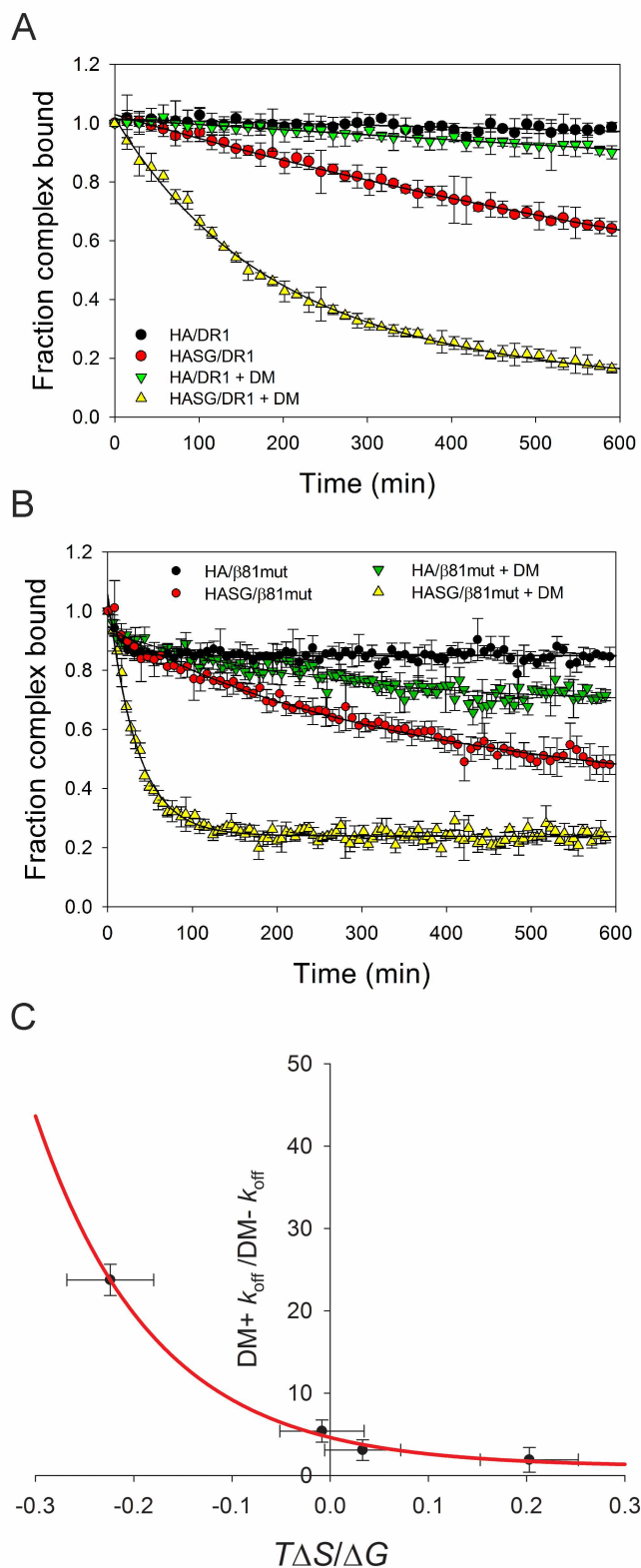
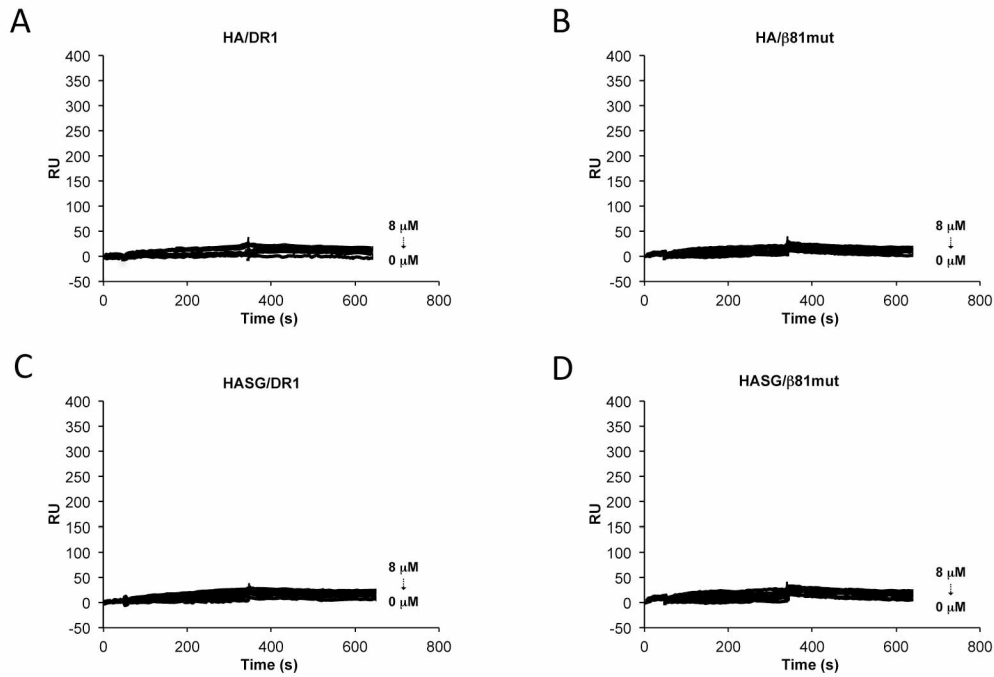


Figure A.6 – FP-based Analysis of DM-susceptibility. Dissociation rates of DR1- (A) and $\beta 81$ mut-peptide complexes (B) in the absence and in the presence of DM. Data are expressed as the fraction of complex remaining relative to $t = 0$. Reactions were performed in triplicate, and data series represent one of three independent experiments. The lines represent the fit of the data to either a one- or a two-phase exponential function. (C) DM-susceptibility of the tested pMHCII complexes, calculated as peptide k_{off} -fold increase, inversely correlates with the restraining of conformational flexibility associated with binding, measured as entropic contribution to free energy decrease. The line represents the fit of the data to a single exponential function.



Supplementary Figure A.1 – SPR Assay of DM Interaction with pMHCII Complexes at pH 7. Affinity measurements were performed by injecting the various pMHCII complexes in two fold dilutions and at seven concentrations from 8 mM and flowing them over DM-coated CM5 sensor chip at flow rate of 5 μ l/min for 5 min and dissociated for 5 min. Binding to DM was analyzed for (A) HA/DR1, (B) HA/b81mut, (C) HASG/DR1, (D) HASG/b81mut. These experiments were repeated three times.

Table A.1: Binding Affinity and Thermodynamic Parameters for each pHLAII dyad tested.

Mutations applied to the HA peptide are in bold.

Complex	Sequence	<i>n</i>	K_D (nM)	DG (kJ mol ⁻¹)	DH (kJ mol ⁻¹)	TDS (kJ mol ⁻¹)
HA/DR1	PKYVKQNTLKLAT	0.93	15.6 ± 1.3	-44.5 ± 1.6	-53.6 ± 0.7	-9.02 ± 0.08
HA/b81mut		0.96	11.2 ± 1.5	-45.4 ± 1.4	-46.9 ± 0.5	-1.50 ± 0.06
HASG/DR1	PKYSKQNTLKL GT	0.98	82.1 ± 6.3	-40.4 ± 1.4	-40.1 ± 0.4	0.34 ± 0.01
HASG/b81mut		0.94	132.5 ± 9.4	-39.2 ± 1.3	-30.5 ± 0.4	8.78 ± 0.11

Table A.2 – Midpoint Temperature, Enthalpy and Heat Capacity of the unfolding transition during thermal denaturation of empty HLAII and HLAII bound to either HA or HASG

Complex	T_m K (°C)	DH_m (kJ mol ⁻¹)	DC_p (kJ mol ⁻¹ K ⁻¹)
Empty DR1	341 (68)	192 ± 8	0.9 ± 0.4
Empty b81mut	341 (68)	188 ± 6	0.9 ± 0.4
HA/DR1	352 (79)	298 ± 15	6.5 ± 1.1
HA/b81mut	349 (76)	310 ± 17	6.1 ± 0.9
HASG/DR1	345 (72)	229 ± 12	4.9 ± 0.6
HASG/b81mut	343 (70)	212 ± 15	5.2 ± 0.7

Reference List

1. Cresswell, P., and P. A. Roche. 2014. Invariant chain-MHC class II complexes: always odd and never invariant. *Immunology and cell biology* 92: 471-472.
2. Reich, M., F. Zou, M. Sienczyk, J. Oleksyszyn, B. O. Boehm, and T. Burster. 2011. Invariant chain processing is independent of cathepsin variation between primary human B cells/dendritic cells and B-lymphoblastoid cells. *Cellular immunology* 269: 96-103.
3. Denzin, L. K., and P. Cresswell. 1995. HLA-DM induces CLIP dissociation from MHC class II alpha beta dimers and facilitates peptide loading. *Cell* 82: 155-165.
4. Stebbins, C. C., M. E. Peterson, W. M. Suh, and A. J. Sant. 1996. DM-mediated release of a naturally occurring invariant chain degradation intermediate from MHC class II molecules. *Journal of Immunology* 157: 4892-4898.
5. Neefjes, J., M. L. Jongsma, P. Paul, and O. Bakke. 2011. Towards a systems understanding of MHC class I and MHC class II antigen presentation. *Nat Rev Immunol* 11: 823-836.
6. Nelson, C. A., and D. H. Fremont. 1999. Structural principles of MHC class II antigen presentation. *Rev Immunogenet* 1: 47-59.
7. Natarajan, S. K., L. J. Stern, and S. Sadegh-Nasseri. 1999. Sodium dodecyl sulfate stability of HLA-DR1 complexes correlates with burial of hydrophobic residues in pocket 1. *J Immunol* 162: 3463-3470.
8. Sato, A. K., J. A. Zarutskie, M. M. Rushe, A. Lomakin, S. K. Natarajan, S. Sadegh-Nasseri, G. B. Benedek, and L. J. Stern. 2000. Determinants of the peptide-induced conformational change in the human class II major histocompatibility complex protein HLA-DR1. *The Journal of biological chemistry* 275: 2165-2173.
9. Tobita, T., M. Oda, H. Morii, M. Kuroda, A. Yoshino, T. Azuma, and H. Kozono. 2003. A role for the P1 anchor residue in the thermal stability of MHC class II molecule I-Ab. *Immunology letters* 85: 47-52.
10. Jardetzky, T. S., J. C. Gorga, R. Busch, J. Rothbard, J. L. Strominger, and D. C. Wiley. 1990. Peptide binding to HLA-DR1: a peptide with most residues substituted to alanine retains MHC binding. *The EMBO journal* 9: 1797-1803.
11. Zarutskie, J. A., R. Busch, Z. Zavala-Ruiz, M. Rushe, E. D. Mellins, and L. J. Stern. 2001. The kinetic basis of peptide exchange catalysis by HLA-DM. *Proceedings of the National Academy of Sciences of the United States of America* 98: 12450-12455.

12. Mellins, E. D., and L. J. Stern. 2014. HLA-DM and HLA-DO, key regulators of MHC-II processing and presentation. *Current opinion in immunology* 26: 115 -122.
13. Anders, A. K., M. J. Call, M. S. Schulze, K. D. Fowler, D. A. Schubert, N. P. Seth, E. J. Sundberg, and K. W. Wucherpfennig. 2011. HLA-DM captures partially empty HLA-DR molecules for catalyzed removal of peptide. *Nature immunology* 12: 54-61.
14. Pos, W., D. K. Sethi, M. J. Call, M. S. Schulze, A. K. Anders, J. Pyrdol, and K. W. Wucherpfennig. 2012. Crystal structure of the HLA-DM-HLA-DR1 complex defines mechanisms for rapid peptide selection. *Cell* 151: 1557-1568.
15. Chou, C. L., and S. Sadegh-Nasseri. 2000. HLA-DM recognizes the flexible conformation of major histocompatibility complex class II. *The Journal of experimental medicine* 192: 1697-1706.
16. Painter, C. A., M. P. Negroni, K. A. Kellersberger, Z. Zavala-Ruiz, J. E. Evans, and L. J. Stern. 2011. Conformational lability in the class II MHC 310 helix and adjacent extended strand dictate HLA-DM susceptibility and peptide exchange. *Proceedings of the National Academy of Sciences of the United States of America* 108: 19329-19334.
17. Guce, A. I., S. E. Mortimer, T. Yoon, C. A. Painter, W. Jiang, E. D. Mellins, and L. J. Stern. 2013. HLA-DO acts as a substrate mimic to inhibit HLA-DM by a competitive mechanism. *Nature structural & molecular biology* 20: 90-98.
18. Ferrante, A., and J. Gorski. 2012. A Peptide/MHCII conformer generated in the presence of exchange peptide is substrate for HLA-DM editing. *Scientific reports* 2: 386.
19. Stern, L. J., J. H. Brown, T. S. Jardetzky, J. C. Gorga, R. G. Urban, J. L. Strominger, and D. C. Wiley. 1994. Crystal structure of the human class II MHC protein HLA-DR1 complexed with an influenza virus peptide. *Nature* 368: 215-221.
20. Imboden, M., D. A. Schaefer, R. D. Bremel, E. J. Homan, and M. W. Riggs. 2012. Antibody fusions reduce onset of experimental *Cryptosporidium parvum* infection in calves. *Veterinary parasitology* 188: 41-47.
21. Sloan, V. S., P. Cameron, G. Porter, M. Gammon, M. Amaya, E. Mellins, and D. M. Zaller. 1995. Mediation by HLA-DM of dissociation of peptides from HLA-DR. *Nature* 375: 802-806.
22. Stern, L. J., and D. C. Wiley. 1992. The human class II MHC protein HLA-DR1 assembles as empty alpha beta heterodimers in the absence of antigenic peptide. *Cell* 68: 465-477.

23. Privalov, P. L., and S. J. Gill. 1988. Stability of protein structure and hydrophobic interaction. *Advances in protein chemistry* 39: 191-234.
24. Bechtel, W. J., and J. A. Schellman. 1987. Protein stability curves. *Biopolymers* 26: 1859-1877.
25. Zarutskie, J. A., A. K. Sato, M. M. Rushe, I. C. Chan, A. Lomakin, G. B. Benedek, and L. J. Stern. 1999. A conformational change in the human major histocompatibility complex protein HLA-DR1 induced by peptide binding. *Biochemistry* 38: 5878-5887.
26. Phillips, J. C., R. Braun, W. Wang, J. Gumbart, E. Tajkhorshid, E. Villa, C. Chipot, R. D. Skeel, L. Kale, and K. Schulten. 2005. Scalable molecular dynamics with NAMD. *Journal of computational chemistry* 26: 1781-1802.
27. Humphrey, W., A. Dalke, and K. Schulten. 1996. VMD: visual molecular dynamics. *Journal of molecular graphics* 14: 33-38, 27-38.
28. Schafer, P. H., J. M. Green, S. Malapati, L. Gu, and S. K. Pierce. 1996. HLA-DM is present in one-fifth the amount of HLA-DR in the class II peptide-loading compartment where it associates with leupeptin-induced peptide (LIP)-HLA-DR complexes. *J Immunol* 157: 5487-5495.
29. Buchli, R., R. S. VanGundy, H. D. Hickman-Miller, C. F. Giberson, W. Bardet, and W. H. Hildebrand. 2005. Development and validation of a fluorescence polarization-based competitive peptide-binding assay for HLA-A*0201--a new tool for epitope discovery. *Biochemistry* 44: 12491-12507.
30. Ferrante, A., and J. Gorski. 2012. Enthalpy-entropy compensation and cooperativity as thermodynamic epiphenomena of structural flexibility in ligand-receptor interactions. *Journal of molecular biology* 417: 454-467.
31. Ferrante, A., and J. Gorski. 2007. Cooperativity of hydrophobic anchor interactions: evidence for epitope selection by MHC class II as a folding process. *J Immunol* 178: 7181-7189.
32. Anderson, M. W., and J. Gorski. 2005. Cooperativity during the formation of peptide/MHC class II complexes. *Biochemistry* 44: 5617-5624.
33. Ferrante, A., M. W. Anderson, C. S. Klug, and J. Gorski. 2008. HLA-DM mediates epitope selection by a "compare-exchange" mechanism when a potential peptide pool is available. *PloS one* 3: e3722.

34. Sato, A. K., T. Sturniolo, F. Sinigaglia, and L. J. Stern. 1999. Substitution of aspartic acid at beta57 with alanine alters MHC class II peptide binding activity but not protein stability: HLA-DQ (alpha1*0201, beta1*0302) and (alpha1*0201, beta1*0303). *Human immunology* 60: 1227-1236.
35. Reich, Z., J. D. Altman, J. J. Boniface, D. S. Lyons, H. Kozono, G. Ogg, C. Morgan, and M. M. Davis. 1997. Stability of empty and peptide-loaded class II major histocompatibility complex molecules at neutral and endosomal pH: comparison to class I proteins. *Proceedings of the National Academy of Sciences of the United States of America* 94: 2495-2500.
36. Rupp, B., S. Gunther, T. Makhmoo, A. Schlundt, K. Dickhaut, S. Gupta, I. Choudhary, K. H. Wiesmuller, G. Jung, C. Freund, K. Falk, O. Rotzschke, and R. Kuhne. 2011. Characterization of structural features controlling the receptiveness of empty class II MHC molecules. *PloS one* 6: e18662.
37. Painter, C. A., A. Cruz, G. E. Lopez, L. J. Stern, and Z. Zavala-Ruiz. 2008. Model for the peptide-free conformation of class II MHC proteins. *PloS one* 3: e2403.
38. Yaneva, R., S. Springer, and M. Zacharias. 2009. Flexibility of the MHC class II peptide binding cleft in the bound, partially filled, and empty states: a molecular dynamics simulation study. *Biopolymers* 91: 14-27.
39. McFarland, B. J., J. F. Katz, A. J. Sant, and C. Beeson. 2005. Energetics and cooperativity of the hydrogen bonding and anchor interactions that bind peptides to MHC class II protein. *Journal of molecular biology* 350: 170-183.
40. Painter, C. A., and L. J. Stern. 2012. Conformational variation in structures of classical and non-classical MHCII proteins and functional implications. *Immunological reviews* 250: 144-157.
41. Bandyopadhyay, A., L. Arneson, C. Beeson, and A. J. Sant. 2008. The relative energetic contributions of dominant P1 pocket versus hydrogen bonding interactions to peptide:class II stability: implications for the mechanism of DM function. *Molecular immunology* 45: 1248-1257.

42. Gupta, S., S. Hopner, B. Rupp, S. Gunther, K. Dickhaut, N. Agarwal, M. C. Cardoso, R. Kuhne, K. H. Wiesmuller, G. Jung, K. Falk, and O. Rotzschke. 2008. Anchor side chains of short peptide fragments trigger ligand-exchange of class II MHC molecules. *PLoS one* 3: e1814.
43. Anderson, M. W., and J. Gorski. 2003. Cutting edge: TCR contacts as anchors: effects on affinity and HLA-DM stability. *J Immunol* 171: 5683-5687.
44. Belmares, M. P., R. Busch, K. W. Wucherpfennig, H. M. McConnell, and E. D. Mellins. 2002. Structural factors contributing to DM susceptibility of MHC class II/peptide complexes. *J Immunol* 169: 5109-5117.
45. Narayan, K., C. L. Chou, A. Kim, I. Z. Hartman, S. Dalai, S. Khoruzhenko, and S. Sadegh-Nasseri. 2007. HLA-DM targets the hydrogen bond between the histidine at position beta81 and peptide to dissociate HLA-DR-peptide complexes. *Nature immunology* 8: 92-100.
46. McFarland, B. J., C. Beeson, and A. J. Sant. 1999. Cutting edge: a single, essential hydrogen bond controls the stability of peptide-MHC class II complexes. *J Immunol* 163: 3567-3571.
47. Stratikos, E., D. C. Wiley, and L. J. Stern. 2004. Enhanced catalytic action of HLA-DM on the exchange of peptides lacking backbone hydrogen bonds between their N-terminal region and the MHC class II alpha-chain. *J Immunol* 172: 1109-1117.
48. Ferrante, A., and J. Gorski. 2010. Cutting Edge: HLA-DM-Mediated Peptide Exchange Functions Normally on MHC Class II-Peptide Complexes That Have Been Weakened by Elimination of a Conserved Hydrogen Bond. *Journal of Immunology* 184: 1153-1158.
49. Zhou, Z., K. A. Callaway, D. A. Weber, and P. E. Jensen. 2009. Cutting edge: HLA-DM functions through a mechanism that does not require specific conserved hydrogen bonds in class II MHC-peptide complexes. *J Immunol* 183: 4187-4191.
50. Doebele, R. C., R. Busch, H. M. Scott, A. Pashine, and E. D. Mellins. 2000. Determination of the HLA-DM interaction site on HLA-DR molecules. *Immunity* 13: 517-527.
51. Busch, R., A. Pashine, K. C. Garcia, and E. D. Mellins. 2002. Stabilization of soluble, low-affinity HLA-DM/HLA-DR1 complexes by leucine zippers. *Journal of immunological methods* 263: 111-121.

52. Yin, L., P. Trenh, A. Guce, M. Wieczorek, S. Lange, J. Sticht, W. Jiang, M. Bylsma, E. D. Mellins, C. Freund, and L. J. Stern. 2014. Susceptibility to HLA-DM is determined by a dynamic conformation of major histocompatibility complex class II molecule bound with peptide. *The Journal of biological chemistry*.
53. Sherman, M. A., D. A. Weber, and P. E. Jensen. 1995. DM enhances peptide binding to class II MHC by release of invariant chain-derived peptide. *Immunity* 3: 197-205.
54. Denzin, L. K., C. Hammond, and P. Cresswell. 1996. HLA-DM interactions with intermediates in HLA-DR maturation and a role for HLA-DM in stabilizing empty HLA-DR molecules. *The Journal of experimental medicine* 184: 2153-2165.
55. Riberdy, J. M., J. R. Newcomb, M. J. Surman, J. A. Barbosa, and P. Cresswell. 1992. HLA-DR molecules from an antigen-processing mutant cell line are associated with invariant chain peptides. *Nature* 360: 474-477.
56. Riberdy, J. M., R. R. Avva, H. J. Geuze, and P. Cresswell. 1994. Transport and intracellular distribution of MHC class II molecules and associated invariant chain in normal and antigen-processing mutant cell lines. *The Journal of cell biology* 125: 1225-1237.
57. Kropshofer, H., A. B. Vogt, L. J. Stern, and G. J. Hammerling. 1995. Self-release of CLIP in peptide loading of HLA-DR molecules. *Science* 270: 1357-1359.

Appendix B

Permission from Lab Collaborators

Approval of work included on thesis

2 messages

Megan Templeton <mltempleton@alaska.edu>
To: "J. Margaret Castellini" <maggie.c@alaska.edu>

Mon, Feb 22, 2016 at 12:13 PM

Hi Maggie,

I was hoping you could approve (in an email back) the work that you were part of that I have included in my thesis. The first is a comparison of DM+ to DM- this is in Table 2.3 on page 39 and referenced in the results on page 28. Also I have included the JI paper as an appendix on page 46. Thank you!

Regards,
Megan Templeton

 **DM Thesis.docx**
6753K

J Margaret Castellini <jcastellini@alaska.edu>
To: Megan Templeton <mltempleton@alaska.edu>

Tue, Mar 1, 2016 at 3:51 PM

Hi Megan,

Yes I am happy to approve your use of those data for your thesis.

It's been a pleasure working with you. Good luck!

MaggieC

[Quoted text hidden]

--

Maggie Castellini
Wildlife Toxicology Lab
Department of Veterinary Medicine
University of Alaska Fairbanks
[907-474-2798](tel:907-474-2798)

Approval of work included in thesis

2 messages

Megan Templeton <mltempleton@alaska.edu>

Mon, Feb 22, 2016 at 12:09 PM

To: Megan Hoffman <mhoffman2@alaska.edu>

Hi Megan,

I was hoping you could approve (in an email back) the work that you were part of that I have included in my thesis. The first is a comparison of DM+ to DM- this is in Table 2.3 on page 39 and referenced in the results on page 28. Also I have included the JI paper as an appendix on page 46. Thanks and I hope everything is going well for you since the vet med program has started!

Regards,
Megan Templeton

 **DM Thesis.docx**
6753K

Megan Hoffman <mhoffman2@alaska.edu>

Tue, Mar 1, 2016 at 4:14 PM

To: Megan Templeton <mltempleton@alaska.edu>

Hi Megan,

Congratulations on finishing! Yes, you have my approval to use the research we worked on together.

See you Thursday at the defense,

Best,

Megan

[Quoted text hidden]

--

Megan Hoffman

Lab Manager
Veterinary Medicine Department
University of Alaska Fairbanks

[\(907\)687-0258](tel:(907)687-0258)